Computer Science • 25(3) 2024 https://doi.org/10.7494/csci.2024.25.3.5811

Saib Bouthina
Mohamed-Rida Abdessemed
Riadh Hocine

CV19T, A NOVEL BIO-SOCIALLY INSPIRED METHOD, BELONGING TO A NEW NATURE-INSPIRED METAHEURISTICS CLASS

Abstract *The paper presents CV19T, a novel bio-socially inspired meta-heuristic, where the cornerstone on which rests is the relationship between humans crowding density, on one side, influenced by their mobility, mutual attractiveness to each other and individual consciousness, and on the other side, the amazing speed of COVID-19 propagation. CV19T originality resides in the fact of combining features from two completely distinct and famous classes, namely: swarm intelligence and Evolutionary Algorithms. Moreover, CV19T extends elitism concept (i.e. survival of the most powerful), on which are based courant evolutionist approaches to the survival of the most beneficial one. Also, CV19T shows that additional parameters can increase control of its behaviour, in many cases, leading to rise in its results relevance. To validate CV19T, it was tested on benchmarks set, including 23 functions (unimodal, multimodal and fixed-dimensional multimodal) and 4 real-world problems.*

Keywords exploration and exploitation, elitism, metaheuristics

Citation Computer Science 25(3) 2024: 351–396

1. Introduction

Nowadays optimization becomes one of the most important research areas. It covers a wide range of techniques and its fields of application are extremely varied, going from routing in all kinds of networks [20, 59], classification [10, 15, 51], data clustering [5, 47], feature selection [45], air traffic control [22, 53], till choose of economic investments [36]. Systems optimization belonging to such kinds of issues makes it possible to find an adequate configuration, to obtain a gain of effort, time, money, energy, and/or satisfaction. For many of these problems, which must be solvable in first, an optimal solution cannot be found by exact methods, because of the prohibitive execution time due to the excessive size of real-world problems [25]. Stochastic optimization refers to methods employed to minimize or maximize objective functions, in the presence of randomness. They are particularly valuable in addressing complex problems where uncertainty plays a significant role [24].

Unlike traditional optimization approaches, these methods are generally meta-heuristics adopting iterative exploratory strategies in order to increase research efficiency in the resolution space. They are soft computing techniques used to find approximate solutions for hard optimization problems, knowing that soft computing is a term applied to a field of computer science that is characterized by the use of inexact computational solutions, for which an exact solution cannot be find in polynomial time [8, 50]. Their adaptability and robustness make them a strong tool in addressing problems characterized by uncertainty and variability [57]. Nature-inspired meta-heuristics is a very investigated sub-domain of meta-heuristics which derives inspiration from diverse natural resources. For instance, Particle Swarm Optimization (PSO) [27] mirrors the collective behavior of flocks, Artificial Bee Colony (ABC) [33] draws from the intelligent foraging strategies of bee colonies, Genetic Algorithms (GA) [4] replicate evolutionary processes, and Ant Colony Optimization (ACO) [42] emulates cooperative foraging mechanisms observed in ant colonies. Recent advancements in this field, exemplified by algorithms like the Walrus Optimization Algorithm (WaOA) [23], Sewing Training-Based Optimization (STBO) [19], and the Osprey optimization algorithm (OOA) [14], underscore the continual evolution and refinement of these methodologies.

This study is motivated by the increasing in complexity as well as the very demanding nature of current theoretical or real optimization problems. Example: In fields as strategic as telecommunication, space, nuclear and aeronautics/naval construction, where inaccuracies in calculations or delays in responses, once-tolerable, can now days have severe consequences [6, 11]. Also, intrinsic limitations of existing optimization methods (see Sub-section 2.4), considered satisfactory in the near past, begins to require a radical change. Lastly, the extraordinary technological evolution in the field of computer science, especially in terms of calculation power, which becomes more and more parallel [1], opens new horizons encouraging to invent new optimization strategies where focus of researchers should shift towards method efficiency, like: optimizing response time and solution quality, rather than to worry about

number of parameters or their intricacies adjustments or other secondary/technical problems [13]. In response to the above-mentioned incitements, while keeping in mind the already cited technological advances, this study introduces a novel optimization method, named CV19T, drawing inspiration from the transmission dynamics of COVID-19, influenced by a set of main factors, namely: the grouping density of humans, their mobility, their attractiveness to each other and the consciousness specific to each of them. Note that several existing algorithms like CHIO [2] and COVIDOA [35] draw inspiration from COVID-19. However, no one of these algorithms is sufficiently competitive (see sub-Section E).

CV19T is a new bio-socially inspired meta-heuristic dealing with difficult problems in the optimization field. The main contributions of this novel approach are:

- Its features are spread over two completely different main classes of nature-inspired meta-heuristics. This combination of characteristics of two classes, already counting among the most powerful in the field of nature-inspired meta-heuristics, has opened a new axis of very promising investigation and gave CV19T a wide range of possibilities, explored and not explored yet, in screening for the best solutions.
- Switch of CV19T from the restricted principle of "survival of the fittest" on which natural evolution is based to a new one: "survival of the most beneficial", where the fittest is not always the most beneficial and its removal is, sometimes, most beneficial than its presence, will open new horizons of investigations. In the context of CV19T, this means that elimination of some best individuals from the previous generation will promote the exploration operation and thereby enhancing the algorithm efficiency.
- An increasing in the parameters number of a given nature-inspired meta-heuristic, by adding adequate new ones, can improve, in many cases, the control of its dynamics and therefore improve the efficiency of this method.

In sum, the main objective of this research is to propose a new nature-inspired meta-heuristic, based on innovative ideas that can open up new avenues for research to resolve hard problems with all their complexity, requirements and constraints, which begin to arise in optimization area. In the future, CV19T have to be improved so that it becomes much more efficient than this current version and thus to be able to meet all the already mentioned expectations.

The rest of this paper is organized as follows: Section 2 conducts a comprehensive literature review by exploring existing works in optimization, in general, and nature-inspired meta-heuristics, in more specific. Also, by locating position of the proposed method within nature-inspired meta-heuristics and highlighting research gaps in this research domain. Section 3 presents conceptual foundation of the proposed method, namely CV19T, including assumptions, model description and related investigations. Section 4 outlines CV19T algorithm, discuss parameters tuning details associated to the proposed algorithm and impact of the chosen configurations on exploration and exploitation mechanisms. Section 5 explains the parameters initialization phase,

introduce the used in comparisons benchmarks and the engineering problems. Afterward, it analyses the obtained results and presents their most important managerial insights. Section 6 resumes the treated problem and motivations of this study, summaries the main obtained results and ends, this conclusion section, by suggesting some future outlooks.

2. Literature review

2.1. Optimization problems

Optimization problems have always been part of our daily life and as time passed some, of the well-studied, of them have become benchmarks, used to test a new proposed methods veracity, like traveling salesman problem (TSP), knapsack problem, MAX-SAT problem and many others [40]. In many cases, optimization problems of today's are part of big projects, which leads to a significant increase in their complexity and requirements making them more and more difficult to solve [25].

Optimization can be defined as the process of determining how to use a given resource most effectively possible while still complying with eventual potential limits, linked to this resource. An optimization problem involves, in this case, seeking the solution that most closely approximates to the optimum of a given objective function describing the use of this resource [12].

2.2. Nature-inspired meta-heuristics

Nature-inspired meta-heuristics and their hybrids have revolutionized algorithm design for solving real-world optimization problems. These methods efficiently explore solution spaces, aiming to strike the optimal balance between exploration and exploitation mechanisms to approach, as closely as possible, exact solutions [44]. These approaches have been successful in various fields, providing efficiency, flexibility, and robustness, and was supposed to meet the complex optimization challenges of the future [49].

Meta-heuristic algorithms can be divided into two big main categories, namely: evolutionary algorithms and swarm intelligence-based [41]. The core operation of evolutionary algorithms involves selecting the strongest individuals for survival and discarding the rest [48]. Swarm intelligence is based, for its part, on cooperative behaviours, taking cues from behaviours of social animals like ants/bees colonies, birds flocks, and fishes schools. At the heart of swarm intelligence concept resides synchronization of movements and collective displacements [9]. Another classification, based on inspiration sources, includes: biology [7], physics [31, 32], chemistry [3, 37], sociology [46], and many other natural resources.

Table 1 illustrates meta-heuristic algorithms categorized according to swarm intelligence and evolutionary algorithm classes. Swarm intelligence algorithms featured in Table 1 include Artificial Bees Colonies (ABC), Ants Colonies Optimization (ACO), COOT optimization, Particle Swarm Optimization (PSO), Osprey Optimization Algorithm (OOA), and Walrus Optimization Algorithm (WaOA).

These algorithms draw inspiration from collective behaviours of various animal species and succeeded to solve diverse optimization problems relating to real-world applications. Specifically, ABC is bio-inspired by the behaviours of honeybees, ACO by the foraging behaviours of ants, COOT by the social behaviours of American coot birds, PSO by the collective flight of birds and collective swimming of fishs, OOA by the natural behaviour of ospreys, and WaOA by the behavioural patterns of walruses in nature.

Table 1

Illustration of meta-heuristic algorithms across various categories and historical areas

Algorithm	Ref	Class	Type	Year	Source of inspiration
Particle Swarm Optimization (PSO)	[34]	Swarm-intelligent	Bio-inspired	1980	Swarms
Ant Colony Optimization (ACO)	[16]	Swarm-intelligent	Bio-inspired	1990	Ant colony
Genetic Algorithm (GA)	[18]	Evolutionary Algorithms	Bio-inspired	1996	Evolution
Artificial Bee colony (ABC)	[29]	Swarm-intelligent	Bio-inspired	2005	Honeybee colony
Imperialist Competitive Algorithm (ICA)	[55]	Evolutionary Algorithms	Socially-inspired	2007	Imperialism
Coronavirus herd immunity optimizer (CHIO)	[2]	Evolutionary Algorithms	Socially-inspired	2021	Herd immunity against coronavirus pandemic (COVID-19)
COOT optimization algorithm (COOT)	[39]	Swarm-intelligent	Bio-inspired	2021	American coot birds
Osprey Optimization Algorithm (OOA)	[14]	Swarm-intelligent	Bio-inspired	2022	The natural behavior of osprey
Coronavirus Optimization Algorithm (COVIDOA)	[35]	Evolutionary Algorithms	Bio-inspired	2022	Coronavirus disease replication lifecycle
Sewing Training-Based Optimization (STBO)	[19]	Evolutionary Algorithms	Socially-inspired	2023	Sewing training
Walrus Optimization Algorithm (WaOA)	[23]	Swarm-intelligent	Bio-inspired	2023	Walrus behaviors in nature

The evolutionary algorithms showcased in Table 1 include the Coronavirus Herd Immunity Optimizer (CHIO), which is socially inspired, and COVIDOA, which is bio-inspired. CHIO focusses on optimizing parameters related to herd immunity and vaccine distribution, drawing inspiration from social behaviours and practices related to public health. In contrast, COVIDOA is inspired by biological processes associated with the spread and evolution of the COVID-19 virus, aiming to optimize parameters related to the development and distribution of COVID-19 vaccines. Finally, STBO takes inspiration from the social context of sewing-training. GA and ICA, two other evolutionary algorithms featured in Table 1, are based on principles of evolution and competition.

In general, Table 1 presents a selection of meta-heuristic algorithms from different historical eras and sources of inspiration, providing a glimpse of the diversity and complexity of these optimization methods.

2.3. Position of the proposed methode

In this study, the authors introduce a novel bio-socio-inspired meta-heuristic called CV19T. It belongs simultaneously to the class of evolutionary algorithms nature-inspired meta-heuristics, as is the case of the famous GA (Genetic Algorithm) method and to the class of swarm-intelligence-based nature-inspired meta-heuristics, as is the case of the famous PSO (Particle Swarm Optimization) method. This makes it exceptionally original, since it benefits from the features of these two very important classes.

1. **Evolutionary Algorithms class:** This first class is characterized by a set of initial populations, constituting the first generation, which will evolve, along a series of generations, to converge, via the considered method (GA for example), towards the best possible solution. In the case of CV19T, each generation contains only one population. By drawing a parallel between CV19T and methods of this first class, it is clear that the population of CV19T is composed of a set of individuals at each generation, who scan the search space progressively. After each well-determined period, individuals among the infected are eliminated and other uninfected are added. This constitutes a new generation which will try to evolve rapidly, towards the best possible solution. The operations used in this case are:
    - **SMB (Survival to the Most Beneficial).** This operation means that every individual within the population can be chosen for removal if it is infected and not beneficial to the community, even if he is among the best/fittest.

      So, in contrast to common practice, certain valuable solutions discovered by infected individuals are deliberately selected for deletion rather than preservation. SMB eliminates these good or promising solutions to give more freedom and slack to the exploration mechanism to express itself without having a negative effect on the exploitation mechanism since several of the best-found solutions are still present.

- **RP (Refreshment and Preservation).** This operation combines refreshment of the population and preservation of its size, which reinforces both exploration and exploitation because the regeneration of the new individuals could be either in promise area or sown randomly within the boundaries of the research space.
- **Contagion.** This operation converts the states of the targeted individuals to pass from the susceptible or normal states to the infected one. With regard to all the infected individuals, this represents a recruitment of newly infected individuals who will come to reinforce the exploitation by intensifying the search around the promising solutions.

2. **Swarm-intelligence-based class:** This second class is characterized by a coordination of individuals' movements, belonging to a given swarm, with a view to scrutinizing the search space in a collective and intelligent manner. This makes it possible to bring out a phenomenon of cooperation at the macrolevel produced because of interactions and exchanges of information between the individual's collective at the micro-level. This search policy increases greatly the convergence chances of the considered method towards the best possible solution and in the shortest possible time.
   PSO remains one of the most interesting examples in this perspective where each particle moves taking into consideration the position of the particle located on the global optimum found so far and the local optimum of its neighbourhood. Similarity with CV19T is direct; individuals of the considered swarm manage to coordinate their movements with respect to each other by bringing out a phenomenon of collective displacement at macroscopic level. This displacement takes place in two phases: any healthy individual is attracted by an infected individual if it is within its scope. On the other hand, this normal individual can resist this attraction by using his own consciousness force. In the second phase, infected individuals are all attracted to the most infected individual and can also resist its attraction force by using their own consciousness force; which amply reinforces the exploitation.
   At the macroscopic level, the observer understands that all these individuals are working in a cooperative manner to converge on the most optimal solution. An individual that is not within the scope of any infected individual is free to move randomly according to the Levy random walk, adapted to the human model, which enhances exploration. The PSO acts in a similar way; each particle must take into account, in its displacement, the position of the best global solution and the best local solutions found in its vicinity.

Also, CV19T draws inspiration from the spread rate of COVID-19 and its correlation with human behaviours. The method incorporates various concepts, such as employing Levy flight to model human displacement, utilizing a stochastic state transformation model (SIR – susceptible, infected, removed), in addition to the two opposing

forces, attractiveness and consciousness, which are mentioned above. Table 2 summarizes the main characteristics and functionalities of CV19T.

Table 2
Recapitulation of main characteristics and functionalities of CV19T

Characteristics		
Name	Description	Inspiration source
Multi-inspiration sources	Leverage strengths of two famous approaches	Swarn Intelligence and Living beings' evolution and adaptation
COVID-19 transmission	Very rapid spread of COVID-19 among humans' gatherings; the more the grouping density of humans increases, the more the propagation speed increases too	Contagious disease transmission and sociology
Balanced research	Good balancing between exploration and exploitation during the search	Nature-inspired meta-heuristics
Attractiveness	Each individual within the population could be attracted to other individuals	Psycho-sociology
Awareness	Force that leads individuals to avoid others in an effort to prevent infection	Psycho-sociology
Humans random walk	Following Levy flight for human displacement	Sociology
Functionalities/Operations		
Name	Description	Inspiration source
SMB (Survival to the Most Beneficial)	Removing some of the promising solutions (most infected individuals) will enhance exploration, which is supposed to reduce the occurrence frequency of the premature convergence phenomenon	Natural evolution
RP (Refreshment and Preservation)	This operation refreshes the current population while preserving its size. This reinforces both exploration and exploitation because the regeneration of the new individuals could be done in promise areas or elsewhere, where they are spread randomly within the boundaries of the research space. This operation maintains population size and balances between exploration/exploitation	Natural evolution
Contagion	This operation concerns the propagation of an infected state which will convert states of near individuals to an infected one to pass from the susceptible or normal states to the infected one. With regard to all the infected individuals, this represents a kind of recruitment of newly infected individuals who will come to reinforce the exploitation by intensifying the search around promising solutions	Contagious disease transmission
Collective displacement	Movements coordination of individuals constituting the considered swarm, with a view to scrutinizing the search space in an efficient manner	School fishes, birds flock, ..., collective intelligence

2.4. Research gaps

This section focuses on the main shortcomings of nature-inspired meta-heuristics used in the study presented in this research work, knowing that these inadequacies concern most nature-inspired meta-heuristics proposed thus far:

1. Despite their parameterization, the resolution scope of nature-inspired meta-heuristics is limited. In many cases, modeling the solution of a given problem using elements provided by a given meta-heuristic can be challenging or even impossible, like in the case of genetic algorithms when it comes to represent the genes in relation with the problem solution.
2. Solutions discovered by nature-inspired meta-heuristics tend to be overly approximate in some cases.
3. Response times can be significant in many instances.
4. Proposed methods are often limited and can only handle problems instances whose sizes are less to a given threshold. For instance, in the case of the Traveling Salesman Problem (TSP), only a certain number of cities can be addressed before the software ceases to function.
5. Quality of the solution found is proportional to the response time consumed to discover it. Developing an approach to decouple solution quality from response time would be an important scientific breakthrough.
6. It is obvious that a large number of parameters associated with a given method increases of its complexity. But this can help, also, in many cases, to control its dynamics, leading thereby to increase its effectiveness. Tempting to control these dynamics in all possible cases will be a good target to reach.
7. Current meta-heuristics lack mechanisms leading to control exploration and exploitation effectively with a view to achieving a more efficiency.
8. Relying on a fixed strategy and constant parameter values restricts the scope of considered nature-inspired meta-heuristics in terms of the problems addressed. Having a dynamic search strategy with adaptable parameter values for different phases of a given meta-heuristic would be highly beneficial.
9. There is a significant research gap in the development of meta-heuristics that integrate inspiration from diverse life areas, such as biology, sociology, psychology, and economy.
10. There is a real lack of theoretical study in the field of meta-heuristics in general and those inspired by nature in particular.
11. Current approaches predominantly focus on one class of meta-heuristics, such as those based on swarm intelligence or evolutionary population dynamics, missing opportunities to leverage synergies arising from combining these different classes.
12. While COVID-19 currently serves as a notable source of inspiration in the field of nature-inspired meta-heuristics, its concepts remain somewhat vague, presenting numerous gaps that hinder more effective exploitation by researchers. For example, statistics studies suggest that various factors, such as blood type, play

a predominant role in COVID-19 spread among humans. However, this remains to be developed further. Once conducted, these studies will likely reinforce the power of meta-heuristics inspired by COVID-19 and may even lead to the proposal of more potent methods.

3. Model description and assumptions

3.1. Effect of people grouping density on infection spread

In the distant past, ancestors of humans lived in small isolated groups, minimizing the spread of infectious diseases unless other agents acted as transmitters. This era, known as "Age of Disaster", encompassed over 99.99% of humanity's history. However, around a hundred thousand years ago, the discovery of agriculture and animal husbandry led to increased human grouping marking the onset of the age of diseases [28]. Despite significant strides in controlling infectious diseases, the 20th century witnessed ongoing threats such as SARS, influenza, antimicrobial-resistant bacteria, Ebola, and measles resurgence [26].

More recently, the emergence of new coronavirus diseases as COVID-19, has underscored the great threat of infectious diseases [17, 54]. It is important to note, for this purpose, that COVID-19 primarily spreads through respiratory droplets and aerosols, emphasizing the importance of maintaining a safe distance from others to mitigate transmission [38].

To show the effect of gatherings on the spread of COVID-19, a stochastic transmission process was studied by expanding the Susceptible-Infected-Removed (SIR) model to human behaviours [30].

In this perspective, the studied population is separated into three compartments: susceptible, infected, and removed, and the stochastic state transformation model SIR is applied.

In Figure B1, the flow allowed to pass from one state of transformation to another is shown. Each hour, transitions from the susceptible state to the infected are computed, with a certain probability while taking into consideration two parameters: the infected rate and the area congestion.

The overall area consists of three zone types: crowded zone, mid zone, and uncrowded zone, each with a different probability of infection defined by the number of people gathered there. The risk of infection at each hour is determined according to Equation (2).

$$P_{infection}(t,d) = P_{zone}(t) R_{infected}(d) \tag{1}$$

$$R_{infected}(d) = \frac{N_{infected}(d)}{N_{infected}(d) + N_{Susceptible}(d)} \tag{2}$$

$P_{zone}(t)$ represents the infection probability at time t in the considered zone, 2% is chosen for $P_{crowdedzone}$, 0.2 % for $P_{mid-zone}$, and 0.02 % for $P_{uncrowdedzone}$.

$R_{infected}(d)$ denotes the percentage of infected by the total number of infected and susceptible by day (d).

"Infected" transfers to "removed" with a certain probability every day, knowing that $R_{removed}(d) = 10\%$ [30].

In the development of CV19T, these probabilities are kept the same as in the original research work on COVID-19 [30]. This decision will ensure that CV19T will conform to the dynamics relating to the concrete infection which happen in the real-world.

3.2. Levy flights for human mobility

Levy flight is the ideal method to look for a target in an unfamiliar area randomly. Many experiments have found that the typical characteristics of Levy flights have been shown in the flight (displacement) behaviour of many animal species and insects. Levy flights are, in general, a sort of random walk, where the steps follow Levy's law of distribution, which can be expressed formally, as shown in Equation (3).

$$L(s) \sim |s|^{-\beta} \tag{3}$$

where s is the step size and $1 < \beta \leq 3$ is an index.

Various studies have shown that human mobility can be defined in terms of Levy flight patterns. A distribution of consistent displacements with Levy flights for human mobility, with $\beta = 1.75 \pm 0.15$, was discovered by Gonzalez and colleagues [21]. This consists of analyzing the mobile phone traces of a set of 10^5 individuals and recording their position every time they receive a phone call or a message.

Levy's walk pattern is based on two main actions, choice of direction, and step length. In CV19T, authors used the Mantegna Levy flight [56], as formulated below:

$$steplenght = \frac{u_j}{v_j}^{1/\beta} \tag{4}$$

$$v_j = \sigma \cdot randn[D] \tag{5}$$

$$u_j = randn[D] \tag{6}$$

Randn[D] represents the normal distribution of dimension D. The parametre σ represents the variance, and it can be calculated as follow:

$$\sigma = \frac{\Gamma(\beta + 1) \cdot sin(\pi \cdot \beta/2)}{\Gamma(\frac{1+\beta}{2}) \cdot \beta \cdot 2^{\frac{\beta-1}{2}}} \tag{7}$$

The parameter Γ represents the Gamma function.

According to the previous equation, the new position calculated basing on levy walk pattern is as follow:

$$x_i^{t+1} = x_i^t + \lambda \cdot steplenght \tag{8}$$

Where λ is the scale factor.

3.3. Exploration and exploitation

Broadly spinking, meta-heuristic algorithms have two basic mechanisms of search to know: exploration and exploitation [44]. Exploration involves searching for solutions in areas of the search space not yet explored, whereas exploitation involves intensify research for solutions in the vicinity of promising regions [52]. In the proposed algorithm, there are 4 possible cases: global exploration, local exploration, global exploitation and local exploitation. These four strategies have been visualized in Figure B2, employing a 2D search space for simplicity, where X and Y axes depict the coordinates of both already existing individuals and those which have just been generated within the search space. In what follows, we will explain each of these 4 cases separately:

1. **Case 1 (Global Exploration).** If individual i is uninfected and not associated with any zone, then it moves randomly (see Figure B2 Case 1) by using levy walk through Equation (8).
2. **Case 2 (Local Exploration).** If individual i is uninfected and belongs to an infected zone, then with probability 0.5, an individual j is selected randomly from this same zone to be used in an updating operation of individual i through Equation (9). As evident from the illustration in Figure B2 case 2, the newly generated solutions lie outside the zone in question. This behaviour mimics the tendency of an individual aiming to evade infection by moving away from the infected area. Moreover, Equation (9) highlights that the primary point of attraction is the origin.

$$individual_i{}^{n+1}.Position = (attractor.Attractiveness - attracted.Awareness)\cdot (attractor.Position - attracted.Position) \tag{9}$$

   The attractor is defined as the individual with the best fitness value between individual i and individual j, while the remaining individual is referred to as the attracted.
3. **Case 3 (Global Exploitation).** If individual i is infected, then it is updated by taking into consideration the Gbest. In this case, attractor is the Gbest, while individual i plays the role of the attracted, and it is updated through Equation (10). The newly generated individuals emerge within the search space between individual i and Gbest as seen in Figure B2 case 3.

$$individual_i^{n+1}.Position = individual_i^n.Position + Step \tag{10}$$

   the parameter $STEP$ is the amount of displacement amount of $individual_i$ toward its attractor and it is calculated by using Equation (11).

$$Step = (attractor.Attractivness - attracted.Awareness)\cdot (attractor.Position - attracted.Position) \tag{11}$$

The parameter *Awareness* is the prevention measures taken by those which are attracted. The parameter *Attractiveness* is the attraction force of the attractor.

$$Attractivness = (\alpha \cdot (|attractor.Cost + tran|/|attracted.Cost + tran|)) \quad (12)$$

The parameter α is used to balance between *Attractiveness* and awareness. The parameter *tran* is a transition, and it used to prevent too small or too big values for *Attractiveness* and it can be calculated as:

$$tran = max(|attractor.Cost, attracted.Cost)| + 1 \quad (13)$$

4. **Case 4 (Local Exploitation).** If individual i is uninfected within a given infected zone, there is a probability of 0.5 that this individual will follow the local best (Lbest) attractor, following Equation (10). In this context, the individual is considered as the attracted party. It is important to note that the emergence of newly generated individuals occurs within the research space between individual i and its attractor, as depicted in Figure B2 under "case 4".

3.4. Spatial grouping

As seen in Figure B3, each infected individual is a center of a circle, called the infected zone.

Individuals within each infected zone are chosen by calculating the Euclidean distance between the above-mentioned infected individual and the rest of the population, knowing that only those who are located inside the aforesaid circle of IR ray are taken into account.

By using the IR (Infection Rayon), update the zone that each individual belongs to. Note that lower IR enhances the diversity, while higher IR enhances convergence since more individuals will enter the infected zone of an infected individual which will increase the number of individuals moving toward their infector (see Sub-section 4.2).

The IR can be calculated by using Equation (14):

$$IR = MaxDistance \cdot P \quad (14)$$

While *distance* is a decimal value between 0 and 1, high *distance* means large IR, while low *distance* means small IR. The maximum distance is calculated by using Equation (15):

$$MaxDistance = Distance(Max, min) \quad (15)$$

Max and Min are tow vectors of size d, designating respectively $UpperBound$ and $LowerBound$.

$$Max = [UB, UB, ...]^d, Min = [LB, LB, ...]^d \quad (16)$$

If an individual is present in two or more zones, it is considered to belong to the zone where the distance to the infector is the shortest among all the zones in question.

The type of a given zone is contingent upon the number of individuals within this zone. For example, a zone containing less or equal to 2 individuals is denoted as an "uncrowded zone", while a zone containing between 3 and 10 individuals is classified as a "mid-zone". Conversely, a zone containing more than 10 individuals is designated as a "crowded zone". These numerical thresholds are adaptable to specific requirements. For example, by elevating the minimum threshold for the categorization of a zone like the one "crowded" the likelihood of potential infection transmission decreases.

This is entirely justifiable, given that the probability of infection transmission is notably higher within crowded zones compared to moderately or slightly overcrowded zones.

In this research, the aforementioned numerical thresholds were meticulously selected through an iterative process involving various permutations. The chosen numerical configuration aligns appropriately with the population size used in this study, containing fifty individuals.

3.5. Assumptions

Assumptions on what the proposed method principle is based can be described as follows:

- COVID-19 virus spreads very rapidly among humans.
- High density of human groupings increases the speed of COVID-19 propagation. There is a proportional relationship between them; higher clustering density leads to increased virus spread.
- Individuals can be attracted to each other for various psycho-sociological reasons: curiosity, inherent human nature of sociability, personal interest towards attractors (e.g., a fan), etc. In this work, what matters is that susceptible individuals are attracted by infected individuals.
- The more individuals are aware of the danger, the more they tend to avoid it; thus, the force of consciousness opposes the force of attraction.
- Human movement, resembling a random pattern to an external observer, adheres to the well-defined mathematical principles of Levy flights.
- Each infected individual has an infection zone with a given range. The solutions space is thus structured into so-called infection zones with different clustering densities.
- Individuals who do not belong to any infection zone are considered as part of the non-infected zone.
- An individual can belong to one or more infection zones or none. If he belongs to multiple infection zones, he is assigned to the one with the closest attractor to him. If the distance is the same for all, one of these infected zones will be selected randomly.

- There are different cases of individual movement including:
  - A susceptible individual located outside all the infection zones will move randomly according to Levy's random walk law adapted to the human model.
  - A susceptible individual located inside a given infection zone will try to flee this zone based on their level of awareness to avoid the infection.
  - An infected individual moves according to the influence exerted on him by the most infected individual of all infection zones (the Gbest).

4. Solution approach

In this section, authors elucidate the strategies employed to address optimization challenges using the proposed nature-inspired meta-heuristic. This segment outlines the algorithm's procedural steps, offering a comprehensive guide for its implementation. Additionally, the discussion includes parameters tuning, ensuring adaptability and robustness across diverse problems.

4.1. Steps of CV19T

1. **Initialization phase**: apart from the parameters fine-tuned in the dedicated Subsection (see Sub-section 4.2), crucial general parameters like population size (NP) and iteration number should be initialized at the beginning.
2. **Evaluation**: In this phase, the fitness function is employed to assess the considered population in order to identify the initial infected individuals. The set of these infected individuals, whose cardinality is IN, contains the highest fitness values, and the highest value among them is saved as Gbest.
3. **End of day:** If (IterationNumber mod DaySize) is different from 0 go to step 7: *this verifies if the day ends or not.*
4. **Remove randomly 10% of infected individuals**: this quantity represents the probability of the removed individuals and is noted $R_{removed}(d)$. To avoid the extinction of the considered population, the removed number of individuals is regenerated in such a way that some of them surround the GBest and the others are spread randomly over the whole of the search space. The state of the regenerated individuals is "susceptible".
5. **Update infection probabilities, via Equation** (1): the infection probability of a given individual depends on the zone type in which it belongs and the total number of infected individuals.
6. **Change the state of the AIN best individuals in the population to "infected"**: to show the propagation of the disease, this algorithm adds, each day, a certain number of infected individuals from the best ones.
7. **Zones creation**: The process of zone creation is accomplished by considering each infected individual as the centre of a circle, constituting what we call "infected zone". Individuals within each infected zone are selected based on their Euclidean distance from the infected individual; only those inside the considered

circle, of Rayon "IR", are taken into account. The number of individuals present in a given zone determines its type. This flexible classification, based on specific needs, aids to understand infection transmission probabilities within each zone type (refer to Sub-Section 3.4 for details).

8. **Update infection state**: In the context of a given population, an individual's state can be either "infected" or "susceptible". The transition from a susceptible state to an infected state is determined through the application of probabilities outlined in step 5. This is done by updating the infection status of each individual within its population. It should be noted that individuals who do not belong to any zone, are classified as part of "uncrowded zone".
9. **Update position**: CV19T is inspired by human displacement causing a crowding phenomenon, facilitating the spread of COVID-19. This displacement is characterized by four distinct cases, each representing a unique strategy for adjusting an individual's position, as detailed in Sub-Section 3.3.
   The exploration process focuses on susceptible individuals and occurs in two ways: firstly, for those who are not assigned to any specific zone and move randomly using the Levy walk law, and secondly, for individuals within an infection zone, who randomly select another individual from the same zone and adapt their search strategy accordingly.
   The exploration goal is to enhance the global search by diversifying the search in order to attempt to reach a comprehensive coverage of the search space.
   On the other hand, exploitation involves some infected-individuals, attracted by the global best and who agree to be attracted (i.e. their own consciousness forces goes in the same direction of the attraction force exercised on them), and also some susceptible-individuals within each infection zone, which are attracted by their infector and who agree to undergo this attractive force
10. **Evaluation**: it consists of using the adequate fitness function, which depends on the problem to solve, in order to evaluate the population, after the updating position of each of its individuals, and return the new global best (GBest), if it exists, and changes its state to "infected" if its sate is "susceptible".
11. **Stop**: This last phase involves the verification conditions forcing the algorithm to halt. Once these conditions are satisfied, this algorithm provides the best solutions found, before stopping. Conversely, if the specified conditions are not met yet, the algorithm will revert to step 3 and resume its iterative execution. The expression of the termination conditions is: "a predefined maximum number of iterations and one of the following sub-conditions: a convergence towards a fixed solution or achievement of an acceptable optimal solution".

The whole process is summarized in Algorithm C3 (see Appendix).

4.2. CV19T parameters tuning

This sub-section concerns parameters of the suggested method (CV19T). Some of these parameters are invented by the authors, which know nothing about their val-

ues. So, this sub-section explains the conduced strategy to find the adequate values of these parameters and show the adopter values of the others parameters already given by other researchers. CV19T's parameter tuning embraces diverse strategies. Key parameters like Levy flight exponent faithfully mirror their real-world counterparts, such as the human random walk pattern, for an authentic representation of natural phenomena. For core elements like the infection probability, CV19T leverages insights gleaned from already established research on COVID-19 transmission rates [30].

This ensures the behaviour of infected individuals, within the algorithm, accurately reflects the virus's spread in the real world, lending a valuable layer of realism and potentially harnessing the intricate dynamics observed in viral propagation.

Additionally, certain parameters are intentionally fixed, in the beginning, by the authors, offering flexibility for adjustments based on the population size. Notably, parameters like the initial infected number ($IN = 1$), day size in term of hours ($DaySize = 24$) and Added Infected Number ($AIN = 3$) are set, initially, by the authors and can be fine-tuned depending on the population size.

Another subset of parameters undergoes a training process, including *Distance*, α *LowerBound* (LB), α *UpperBound* (UB), *Awareness LB*, *Awareness UB*, λ *LB* and λ *UB*, emphasizing the adaptability and precision of CV19T in the capture of the complex-optimization-landscapes dynamics.

For the adjustment of CV19T algorithm parameters, various settings are considered, presented as scenarios (refer to Table 3).

Table 3
Parameters tuning scenarios

		Distance	α LB	α UB	Awareness LB	Awareness UB	λ LB	λ UB
Scenario 1	Awareness	0.1	0	2	0	1	1	2
Scenario 2		0.1	0	2	1	2	1	2
Scenario 3		0.1	0	2	0	0.1	1	2
Scenario 4		0.1	0	2	0	0.01	1	2
Scenario 5		0.1	0	2	0	0.001	1	2
Scenario 6	λ	0.1	0	2	0	0.1	0	2
Scenario 7		0.1	0	2	0	0.1	0	1
Scenario 8		0.1	0	2	0	0.1	1	2
Scenario 9	α	0.1	0	2	0	0.1	1	2
Scenario 10		0.1	0	1	0	0.1	1	2
Scenario 11		0.1	1	2	0	0.1	1	2
Scenario 12	P	0.01	1	2	0	0.1	1	2
Scenario 13		0.3	1	2	0	0.1	1	2
Scenario 14		0.7	1	2	0	0.1	1	2
Scenario 15		1	1	2	0	0.1	1	2

To select the best parameters values, the CV19T algorithm is tested on 6 benchmarks (see Sub-Section 5.2). Among these benchmarks, 2 are unimodal (F1, F6), 2 are multimodal (F10, F12), and 2 are fixed-dimensional (F14, F19). Evaluation of each scenario involves the execution of the concerned algorithm 5 times in a row,

and this independently, to mitigate the impact of chance on the results. Subsequently, the mean value is calculated to facilitate comparison. This methodology empowers the authors to ascertain the most suitable parameter configuration for CV19T algorithm.

Table 4 presents the outcomes obtained by applying different parameters scenarios to the targeted benchmarks. The results indicate that scenario 3 yields the most favourable results in terms of *Awareness*. Consequently, the appropriate range for the *Awareness* parameter (*Awareness*) falls between 0 and 0.1.

Regarding the λ parameter, which serves as the step size for Levy walk displacement, scenario 8 exhibits the optimal parameter configuration, with λ ranging between 1 and 2.

For the α parameter, scenario 11 demonstrates the best performance, suggesting that α should be set within the range of 1 to 2.

Table 4
Parameters tuning results

		F01	F06	F10	F12	F14	F19
Scenario 1		1.60E+03	2.35E+03	1.52E+01	2.01E+06	**3.55E+00**	–3.85E+00
Scenario 2		2.14E+04	2.54E+04	1.47E+01	1.39E+08	8.77E+00	–3.54E+00
Scenario 3	Awareness	3.52E+02	**3.82E+02**	**1.28E+01**	7.24E+01	5.33E+00	**–3.86E+00**
Scenario 4		**1.41E+02**	6.56E+02	1.65E+01	5.55E+03	8.21E+00	**–3.86E+00**
Scenario 5		2.69E+02	5.76E+02	1.48E+01	**4.89E+01**	7.80E+00	**–3.86E+00**
Scenario 6		7.92E+02	2.76E+03	**1.19E+01**	6.40E+02	**7.27E+00**	**–3.86E+00**
Scenario 7	α	8.61E+02	1.35E+03	1.46E+01	2.20E+03	9.69E+00	**–3.86E+00**
Scenario 8		**2.19E+02**	**6.51E+02**	1.46E+01	**6.87E+01**	8.34E+00	**–3.86E+00**
Scenario 9		1.97E+02	3.80E+02	**1.54E+01**	2.23E+04	6.10E+00	**–3.86E+00**
Scenario 10	λ	1.07E+04	1.48E+04	1.59E+01	2.32E+07	**4.36E+00**	–3.83E+00
Scenario 11		**1.12E+02**	**2.34E+02**	1.90E+01	**1.24E+02**	5.31E+00	**–3.86E+00**
Scenario 12		1.56E+02	6.35E+01	1.88E+01	2.87E+03	6.30E+00	**–3.86E+00**
Scenario 13	P	3.14E+02	3.22E+02	1.76E+01	6.81E+02	1.17E+01	**–3.86E+00**
Scenario 14		**0.00E+00**	**1.68E–03**	**8.88E–16**	4.56E-04	3.17E+00	**–3.86E+00**
Scenario 15		**0.00E+00**	**1.69E–03**	**8.88E–16**	**1.67E–04**	**1.39E+00**	**–3.86E+00**

In the case of the *Distance* parameter used to define the infection radius, the value of 1 is considered appropriate. Figure 1 showcases the exploration and exploitation behaviour of CV19T algorithm in different scenarios. In this representation, the X-axis denotes the iteration count, whereas the Y-axis denotes the count of individuals engaged in exploration and exploitation during each iteration.

Scenarios 1 to 13 show an imbalance between the exploration and exploitation mechanisms. Conversely, scenarios 14 and 15 exhibit an interesting balance between these two mechanisms, which helps to elucidate the results presented in Table 4.

Furthermore, the parameter P exerts a significant influence over the equilibrium between exploration and exploitation. This observation is drawn from the analysis of Scenarios 12, 13, 14, and 15.

Specifically, it is discernible that when P assumes smaller values (as depicted in Figure 1 for Scenarios 12 and 13), a greater proportion of individuals within the system engage in exploration activities, as evidenced by the corresponding curves. However, as the value of parameter P is increased, it is noted a growth in the number of individuals participating in both exploration and exploitation.
This rise is, notably, accompanied by a prevalence of oriented exploitation activities (see the Scenarios 14 and 15 in Figure 1).

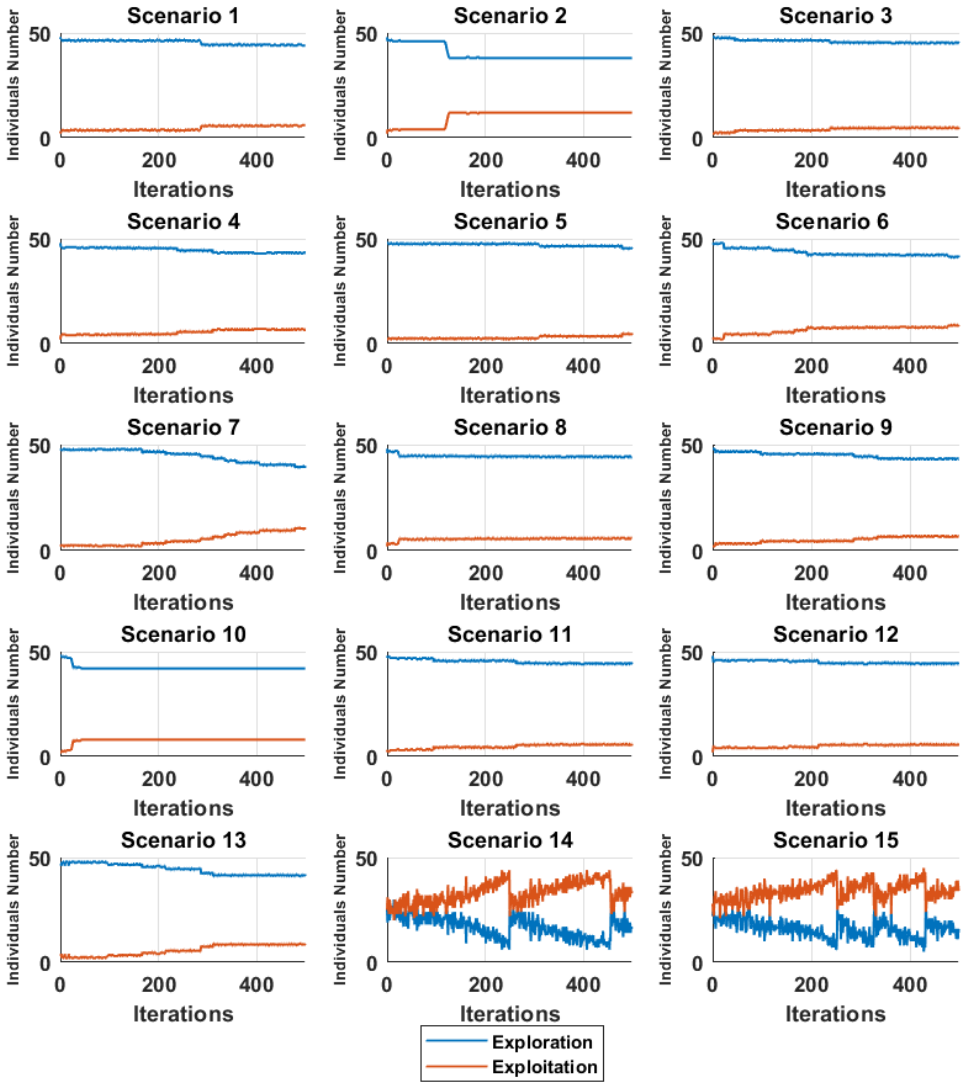

Figure 1. Exploration and exploitation rates basing on different settings

5. Results and discussion

Data analysis plays a pivotal role in assessing the performance and effectiveness of meta-heuristic algorithms, particularly when comparing and evaluating their outcomes. By employing rigorous data analysis techniques, we gain insights into the strengths and weaknesses of each meta-heuristic, facilitating a comprehensive understanding of their behavior across diverse scenarios. Furthermore, the application of data analysis is essential in discerning the meta-heuristic's adaptability to both standardized benchmark functions and real-life engineering problems, providing valuable information for researchers and practitioners to make informed decisions on algorithm selection and implementation.

This section encompasses the results derived from applying the proposed method to both benchmark functions and real-life engineering problems. The comprehensive data analysis not only unveils the algorithm's performance metrics but also provides managerial insights, offering practical implications for decision-makers in choosing and implementing meta-heuristic algorithms in various applications.

5.1. Parameter settings for the 8 algorithms used in comparison

To assess the competitiveness of the proposed meta-heuristic, a comparative analysis was conducted against 8 meta-heuristics originating from various historical areas and different sources of inspiration. This sub-section concerns parameters of the 8 chosen reference-methods for the results comparisons stage; values of these parameters are already established by other researchers. These reference-methods included ABC (Artificial Bee Colony), ACO (Ant Colony Optimization), CHIO (Coronavirus Herd Immunity Optimizer), COOT, COVIDOA (COVID-19 Inspired Optimization Algorithm), GA (Genetic Algorithm), ICA (Imperialist Competitive Algorithm), and PSO (Particle Swarm Optimization).

For each of these meta-heuristics, two types of parameters were considered: general parameters and algorithm-specific parameters. General parameters encompass factors such as population size, number of iterations, and problem dimension. In these conditions, the general parameter values were set as follows: population size = 50, iteration number = 10.000, and problem dimension (applicable to a non-fixed dimensional problems) = 30.

To ensure a fair comparison, each algorithm was executed 20 times in a row, and this independently of each other. Specific settings, for each algorithm, were outlined in Table A1 (see Appendix). Note that all specific parameters referring to CV19T algorithm were gathered in Sub-section 4.2.

5.2. Benchmark functions

Unimodal benchmarks are mathematical functions with only one global optimum, this means that only one point in the function's domain gives the highest value. Such functions are helpful in testing the exploitation ability of nature-inspired meta-heuristics,

i.e. their ability to converge towards the global optimum. On the other hand, multimodal benchmarks are mathematical functions with multiple local optima, this means that various points in the function's domain can give relatively high values. These functions are helpful in testing the exploration ability of optimization algorithms, i.e. their ability to find diverse solutions and avoid getting trapped in a given local optima.

By using both unimodal and multimodal benchmarks, researchers can assess the overall performance of targeted optimization algorithms by evaluating their ability to converge to the global optimum while avoiding getting trapped in any local optimum.

In this work, CV19T is tested using 7 unimodal benchmarks (see Appendix Figure D1), 6 multimodal (see Appendix Figure D2) and 10 fixed-dimensional multimodal benchmarks (see Appendix Figure D3). Fixed-dimensional multimodal benchmarks encompass multi-modal benchmark functions characterized by unchanging dimensions. These benchmarks are also harnessed to evaluate the efficacy of exploration strategies.

5.2.1. Results for benchmark functions

Comparative outcomes of the proposed algorithm in relation with 8 other methods are showcased in Tables E1, E2, E3 and E4 (see Appendix). The results are expressed in statistical terms of the best (BEST), mean (MEAN), worst (WORST), standard deviation (STD) values and have been analysed by using the statistical approach named: "two-tailed t-test". During the t-test analysis, results of the proposed method are compared with each of the aforementioned reference algorithms. The outcome of this comparison is assessed by using null hypothesis H0 and alternative hypothesis H1. H0 refers to the null hypothesis and means that no significant difference exists between the compared algorithms. On the other hand, H1 refers to the alternative hypothesis, which goes against the hypothesis H0 In this practical phase, the two hypothesis forms were utilized.

Table E1 presents the outcomes obtained by using unimodal benchmarks to assess the exploitation ability of the proposed algorithm. It is evident from table E1 that CV19T algorithm achieved the highest results across all the unimodal benchmarks, demonstrating its exceptional performance. Notably, CV19T successfully reached the exact solution in 5 out of 7 benchmarks, providing strong evidence of the proposed algorithm's robust exploitation capability. The COOT algorithm is in the second position by obtaining the best results in 4 out of 7 benchmarks. However, CV19T exhibits superior performance in terms of standard deviation (STD) values, which indicates that it is more suitable for this kind of optimisation problems. According to t-test results, it is obvious that CV19T behaviours are very close to those of COOT, while they differ greatly from those of ACO and CHIO.

Table E2 presents the outcomes obtained from testing multimodal benchmarks to assess the exploration ability of the proposed algorithm. Based on the obtained results, CV19T chows its superiority on the other methods in the resolution of the

6 considered benchmarks. ICA followed in second position with a score of 4 out of 6 benchmarks, while sharing with CV19T the two highest performances. Among the 6 used benchmarks, CV19T was found to be the more suitable in three functions (F09, F10, and F11), while ICA was deemed more suitable in the remaining benchmarks. COOT algorithm came in third position, sharing the highest scores in 3 benchmarks with CV19T, but it was considered, overall, the less suitable. The remaining algorithms exhibited similar medium performances, except for COVIDOA and GA, which was the less successful.

Results of the two-tailed t-test indicate that there is a significant difference in performance between CV19T and the other algorithms. The alternative hypothesis H1 is supported for most algorithms across all benchmarks, stipulating that their own performances differ significantly from those of CV19T, except that CV19T exhibits a noticeable similarity with PSO.

For the fixed-dimensional multi-modal benchmarks, the results obtained by the various algorithms appear to be closely aligned. More precisely, CV19T, COOT, ICA, and PSO achieve the best performances for all the benchmarks (10/10). Notably, CV19T and COOT exhibit higher suitability based on the MEAN WORST and STD results. The remaining algorithms performed also well, securing a more than good rankings (with 9 out of 10 benchmarks, except of F15). The COVIDOA algorithm, however, came last by succeeding only in 8 out of 10 benchmarks.

Two-tailed t-test allowed to come out with the similarities, in matter of performances, between CV19T and ACO (7 out of 10 benchmarks). Conversely, CV19T demonstrated significant dissimilarity with both CHIO and COVIDOA, highlighting thereby the distinctiveness of this algorithm from the other algorithms inspired of COVID-19.

These findings shed light on the hard competitiveness of CV19T, COOT, ICA, and PSO algorithms in achieving top results in solving the targeted benchmarks. Furthermore, the t-test analysis underscores the unique characteristics of CV19T when compared to the other COVID-19-inspired algorithms.

The convergence curves of the compared algorithms relating to the targeted unimodal and multimodal benchmarks are illustrated, respectively, in Figure F1 and F2 (see Appendix). In this representation, the X-axis corresponds to the iteration count, while the Y-axis signifies the lowest cost discovered during each iteration (the same for Figure F3 and F4). A careful graphs analysis reveals distinct patterns: Firstly, CV19T exhibits an exceptional convergence rate, as its curve remains almost stick to the X-axis along all benchmarks except for F8. This indicates that CV19T converges rapidly towards optimal solutions. On the other hand, ABC and CHIO display a moderate convergence speed, as their curves show a gradual decline towards X-axis. ACO, however, exhibits the slowest convergence speed among all the used algorithms, as its curve takes a longer time to approach the X-axis. The remaining algorithms demonstrate a convergence speed close to that of CV19T, which testify their ability to quickly move towards optimal solutions.

Figure F3 (see Appendix) showcases the convergence curves of the algorithms for fixed dimensional multimodal benchmarks. A comprehensive analysis of the graph reveals several key observations. In most cases, the algorithms exhibit similar convergence speeds. However, for benchmark F21, COOT and ICA display the fastest convergence rates, indicating their ability to quickly approach optimal solutions. Conversely, ACO, GA, and COVIDOA demonstrate the slowest convergence speeds for this benchmark. The remaining algorithms, including CV19T, exhibit a medium level of performance.

Moving on to benchmark F22, ABC, COOT, GA, and ICA stand out with the fastest convergence rates. Conversely, PSO displays the lowest convergence rate among all the algorithms. The rest of the algorithms demonstrate a medium level of convergence performance for this benchmark. For benchmark F23, CV19T, ABC, COOT, COVIDOA, and ICA showcase the fastest convergence speeds, indicating their efficiency in converging towards optimal solutions. On the other hand, ACO and GA exhibit the lowest convergence rates. PSO and CHIO display a medium convergence speed for this particular benchmark.

Figure F3 highlights the varying convergence speeds of the algorithms for fixed dimensional multimodal benchmarks. While some algorithms perform well others are bad, according to the targeted benchmark. Broadly speaking, the algorithms majority show medium convergence performance, with a few outliers demonstrating exceptionally fast or slow convergence rates depending on the considered benchmark.

5.3. Real-life engineering problems

CV19T algorithm was utilized to solve 4 engineering problems, namely: the Three Bar Truss Design (TBTD), Stepped Cantilever Beam Design (SCBD), Multiple Disc Clutch Brake Design (MDCBD), and Hydrodynamic Thrust Bearing Design (HTBD) (see Appendix Figure B4) [58] [43]. In the TBTD problem (see Figure B4a), there are 2 parameters to optimize, namely A1 and A2. In SCBD problem, there are 10 parameters to optimize, as depicted B4b. MDCBD problem has 4 parameters to optimize (see Figure B4c), and finally, HTBD problem has 4 parameters to optimize (see Figure B4d). It is noteworthy that all these problems were formulated as optimization problems to minimize.

5.3.1. Results for real-life engineering problems

Table E5 (see Appendix) illustrates the outcomes obtained when applying CV19T and the other aforementioned methods to solve the 4 engineering problems. Overall, all the algorithms produced close results, except for MDCBD where CV19T clearly outperformed them all, demonstrating thus its superiority.

For the HTBD problem, it is interesting to observe that ICA algorithm delivered the fastest result in terms of the BEST-criterion, but it fails in terms of suitability for other aspects of the problem.

To evaluate the performance of the other algorithms relative to CV19T, a two-tailed t-test was carried out. The obtained results indicate that most algorithms exhibited similar performance to CV19T for the SCBD and HTBD problems, which suggests that they are statistically comparable. However, the CHIO algorithm deviated from this trend to verify the alternative hypothesis. On the other hand, when examining the TBTD and MDCBD problems, most of the reference-algorithms, used in this study, verified the alternative hypothesis, indicating a significant difference in performance when compared with CV19T.

In this perspective, Figure F4 (see Appendix) showcases the curves behaviours of all these reference-algorithms at time of their resolution of all the targeted problems.

It is evident, from Figure F4, that the convergence speeds of TBTD, SCBC, and HTBD are comparable. However, when analysing MDCBD, it becomes apparent that both CV19T and ICA exhibit the most rapid convergence, yielding the most favourable outcomes. On the other hand, COVIDOA displays the slowest convergence speed when solving MDCBD. As for the remaining methods, their convergence speeds are relatively similar.

5.4. Managerial insights

- CV19T application to the 4 targeted engineering problems, producing competing solutions to some famous methods, shows its real efficiency. This practical success underlines that CV19T is already ready to be used to solve real-world problems.
- The proposed approach will open, certainly, a new avenue for combining between features of several distinct classes of nature-inspired meta-heuristics to spawn entirely new meta-heuristic type, leveraging the strength of the combined classes. This operation different entirely from hybridization principal.
- Authors of this research work invented a new operator concerning the evolutionary approaches class, which generalizes the "survival of the fittest" principal to the "survival of the most beneficial" principal. This idea will surely be widely used in future research works relating to meta-heuristics based on the population evolution.
- Authors have shown, in this study, that adding new adequate parameters has increased, in many cases, the dynamics control of CV19T to make it more effective (see Appendix Table A2). In this perspective, they believe that this finding can be generalized by trying to find even better parameter values than those already found. This will open up a new research axis, pushing researchers to try to increase the efficiency of existing meta-heuristics by adding adequate parameters to them and adjusting their values as appropriate.

6. Conclusion

Current optimization problems become increasingly difficult to solve while presenting very hard constraints and requirements that even nature-inspired meta-heuristics

which count between the most performant existing methods to solve them begin to find serious difficulties to deal with. To fill this increasingly gap, the solution addressed in this research work is to suggest a novel bio-socio-inspired meta-heuristic aiming to compete with the famous, powerful or alike type methods in the field of nature-inspired metaheuristics.

Given that the field of nature-inspired metaheuristics is currently the most popular in terms of solving difficult optimization problems, because of the satisfactory results they have provided in the near past, it is obvious that this represents a fairly strong motivation encouraging authors to start their research work by taking this metaheuristics-sub-domain as a starting point. CV19T has proven to be as consistent and efficient as the carefully selected nature-inspired meta-heuristics used in the comparative study. In many cases, conducted statistical analysis revealed the superiority of the proposed algorithm in terms of convergence speed and quality of found solutions, and even it manages to discover, sometimes, the exact solutions. On the other hand, the results related to the experienced engineering problems testify the promising future of CV19T in solving real-world problems. Through this research, the authors have opened a new avenue of investigation by demonstrating the possibility of combining characteristics of two completely different classes of nature-inspired metaheuristics to propose a new powerful method. In addition, the concept of "survival of the most beneficial" generalized to this of "survival of the fittest" will undoubtedly be adopted in future researches relating to the evolutionary approaches. Also, adding new adequate parameters will be a new investigation direction to improve the control and increase the performances of existing meta-heuristics.

In the near future, the authors planned to use CV19T to solve challenging theoretical problems, such as the Traveling Salesman Problem, while trying to surpass the results obtained so far, and also real-world problems, related to domains as strategic as digital image processing, cryptography, wireless networks, collective robotics, and swarms of drones. Refinements and improvements to the CV19T meta-heuristic and more judicious adjustments to its parameters will be necessary in this case.

References

[1] Ajani S.N., Khobragade P., Dhone M., Ganguly B., Shelke N., Parati N.: Advancements in Computing: Emerging Trends in Computational Science with Next-Generation Computing, *International Journal of Intelligent Systems and Applications in Engineering*, vol. 12(7S), pp. 546–559, 2024. https://ijisae.org/index.php/IJISAE/article/view/4159.

[2] Al-Betar M.A., Alyasseri Z.A.A., Awadallah M.A., Abu Doush I.: Coronavirus herd immunity optimizer (CHIO), *Neural Computing and Applications*, vol. 33, pp. 5011–5042, 2021. doi: 10.1007/s00521-020-05296-6.

[3] Alatas B.: A novel chemistry based metaheuristic optimization method for mining of classification rules, *Expert Systems with Applications*, vol. 39(12), pp. 11080–11088, 2012. doi: 10.1016/j.eswa.2012.03.066.

[4] Alhijawi B., Awajan A.: Genetic algorithms: theory, genetic operators, solutions, and applications, *Evolutionary Intelligence*, vol. 17, pp. 1245–1256, 2024. doi: 10.1007/s12065-023-00822-6.

[5] Ariyaratne A., Ilankoon I., Samarasinghe U., Silva R.: Finding Playing Styles of Badminton Players Using Firefly Algorithm Based Clustering Algorithms: Finding Playing Styles of Badminton Players Using FA Varients, *Computer Science*, vol. 24(3), 2023. doi: 10.7494/csci.2023.24.3.5116.

[6] Bhandari S., Sahay K.B., Singh R.K.: Optimization Techniques in Modern Times and Their Applications. In: *2018 International Electrical Engineering Congress (iEECON)*, pp. 1–4, 2018. doi: 10.1109/IEECON.2018.8712308.

[7] Binitha S., Sathya S.S.: A Survey of Bio inspired Optimization Algorithms, *International Journal of Soft Computing and Engineering*, vol. 2(2), pp. 137–151, 2012. https://www.ijsce.org/portfolio-item/B0523032212/.

[8] Blum C., Roli A.: Metaheuristics in combinatorial optimization: Overview and conceptual comparison, *ACM Computing Surveys (CSUR)*, vol. 35(3), pp. 268–308, 2003. doi: 10.1145/937503.937505.

[9] Chakraborty A., Kar A.K.: Swarm Intelligence: A Review of Algorithms. In: *Nature-Inspired Computing and Optimization: Theory and Applications*, pp. 475–494, Springer, 2017. doi: 10.1007/978-3-319-50920-4_19.

[10] Chola Raja K., Kannimuthu S.: Deep learning-based feature selection and prediction system for autism spectrum disorder using a hybrid meta-heuristics approach, *Journal of Intelligent & Fuzzy Systems*, vol. 45(1), pp. 797–807. doi: 10.3233/jifs-223694.

[11] Conway B.A., Paris S.W.: Spacecraft Trajectory Optimization Using Direct Transcription and Nonlinear Programming. In: B.A. Conway (ed.), *Spacecraft Trajectory Optimization*, pp. 37–78, Cambridge Aerospace Series, Cambridge University Press, 2010. doi: 10.1017/CBO9780511778025.004.

[12] De León-Aldaco S.E., Calleja H., Alquicira J.A.: Metaheuristic optimization methods applied to power converters: A review, *IEEE Transactions on Power Electronics*, vol. 30(12), pp. 6791–6803, 2015. doi: 10.1109/tpel.2015.2397311.

[13] Deb K.: Multi-objective optimisation using evolutionary algorithms: an introduction. In: L. Wang, A.H.C. Ng, K. Deb (eds.), *Multi-objective Evolutionary Optimisation for Product Design and Manufacturing*, pp. 3–34, Springer, London, 2011. doi: 10.1007/978-0-85729-652-8_1.

[14] Dehghani M., Trojovskỳ P.: Osprey optimization algorithm: A new bio-inspired metaheuristic algorithm for solving engineering optimization problems, *Frontiers in Mechanical Engineering*, vol. 8, 1126450, 2023. doi: 10.3389/fmech.2022.1126450.

[15] Dhief I., Feroskhan M., Alam S., Lilith N., Delahaye D.: Meta-Heuristics Approach for Arrival Sequencing and Delay Absorption Through Automated Vectoring. In: *2023 IEEE Congress on Evolutionary Computation (CEC)*, pp. 1–8, IEEE, 2023. doi: 10.1109/cec53210.2023.10254077.

[16] Dorigo M., Birattari M., Stützle T.: Ant colony optimization, *IEEE Computational Intelligence Magazine*, vol. 1(4), pp. 28–39, 2006. doi: 10.1109/MCI.2006.329691.

[17] Fan Y., Zhao K., Shi Z.L., Zhou P.: Bat coronaviruses in China, *Viruses*, vol. 11(3), 210, 2019. doi: 10.3390/v11030210.

[18] Forrest S.: Genetic algorithms, *ACM Computing Surveys (CSUR)*, vol. 28(1), pp. 77–80, 1996. doi: 10.1145/234313.234350.

[19] Ghadimi N., Yasoubi E., Akbari E., Sabzalian M.H., Alkhazaleh H.A., Ghadamyari M.: SqueezeNet for the forecasting of the energy demand using a combined version of the sewing training-based optimization algorithm, *Heliyon*, 2023. doi: 10.1016/j.heliyon.2023.e16827.

[20] Gomes R., Vieira D., de Castro M.F.: Application of Meta-Heuristics in 5G Network Slicing: A Systematic Review of the Literature, *Sensors*, vol. 22(18), 6724, 2022. doi: 10.3390/s22186724.

[21] González M.C., Hidalgo C.A., Barabási A.L.: Understanding individual human mobility patterns, *Nature*, vol. 458(7196), pp. 779–782, 2008. doi: 10.1038/nature07850.

[22] Grishin I.Y., Timirgaleeva R.R.: Air navigation: Optimisation control ofmeans cueing of the air-traffic control system. In: *2017 21st Conference of Open Innovations Association (FRUCT)*, pp. 134–140, IEEE, 2017. doi: 10.23919/fruct.2017.8250175.

[23] Han M., Du Z., Yuen K.F., Zhu H., Li Y., Yuan Q.: Walrus optimizer: A novel nature-inspired metaheuristic algorithm, *Expert Systems with Applications*, vol. 239, 122413, 2023. doi: 10.1016/j.eswa.2023.122413.

[24] Hannah L.A.: Stochastic optimization. In: J.D. Wright (ed.), *International Encyclopedia of the Social & Behavioral Sciences (Second Edition)*, pp. 473–481, Elsevier London, England, 2015. doi: 10.1016/b978-0-08-097086-8.42010-6.

[25] Harsha P., Charikar M., Andrews M., Arora S., Khot S., Moshkovitz D., Zhang L., *et al.*: Limits of Approximation Algorithms: PCPs and Unique Games (DIMACS Tutorial Lecture Notes), *arXiv preprint arXiv:10023864*, 2010. doi: 10.48550/arXiv.1002.3864.

[26] Hoang T., Coletti P., Melegaro A., Wallinga J., Grijalva C.G., Edmunds J.W., Beutels P., Hens N.: A systematic review of social contact surveys to inform transmission models of close-contact infections, *Epidemiology (Cambridge, Mass)*, vol. 30(5), 723, 2019. doi: 10.1097/ede.0000000000001047.

[27] Jain M., Saihjpal V., Singh N., Singh S.B.: An overview of variants and advancements of PSO algorithm, *Applied Sciences*, vol. 12(17), 8392, 2022. doi: 10.3390/app12178392.

[28] Jones S.: *Germs, Genes and Genesis: The History of Infectious Disease*, Gresham College, 2016.

[29] Karaboga D.: Artificial bee colony algorithm, *Scholarpedia*, vol. 5(3), 6915, 2010. doi: 10.4249/scholarpedia.6915.

[30] Karako K., Song P., Chen Y., Tang W.: Analysis of COVID-19 infection spread in Japan based on stochastic transition model, *Bioscience trends*, 2020. doi: 10.5582/bst.2020.01482.

[31] Kaveh A., Akbari H., Hosseini S.M.: Plasma generation optimization: a new physically-based metaheuristic algorithm for solving constrained optimization problems, *Engineering Computations*, 2020. doi: 10.1108/ec-05-2020-0235.

[32] Kaveh A., Bakhshpoori T.: Water evaporation optimization: a novel physically inspired optimization algorithm, *Computers & Structures*, vol. 167, pp. 69–85, 2016. doi: 10.1016/j.compstruc.2016.01.008.

[33] Kaya E., Gorkemli B., Akay B., Karaboga D.: A review on the studies employing artificial bee colony algorithm to solve combinatorial optimization problems, *Engineering Applications of Artificial Intelligence*, vol. 115, 105311, 2022. doi: 10.1016/j.engappai.2022.105311.

[34] Kennedy J., Eberhart R.: Particle swarm optimization. In: *Proceedings of ICNN'95 – International Conference on Neural Networks*, vol. 4, pp. 1942–1948, IEEE, 1995. doi: 10.1109/ICNN.1995.488968.

[35] Khalid A.M., Hosny K.M., Mirjalili S.: COVIDOA: a novel evolutionary optimization algorithm based on coronavirus disease replication lifecycle, *Neural Computing and Applications*, vol. 34(24), pp. 22465–22492, 2022. doi: 10.1007/s00521-022-07639-x.

[36] Krasovskii A.A., Taras'ev A.M.: Dynamic optimization of investments in the economic growth models, *Automation and Remote Control*, vol. 68(10), pp. 1765–1777, 2007. doi: 10.1134/S0005117907100050.

[37] Lam A.Y.S., Li V.O.K.: Chemical-reaction-inspired metaheuristic for optimization, *IEEE Transactions on Evolutionary Computation*, vol. 14(3), pp. 381–399, 2009. doi: 10.1109/tevc.2009.2033580.

[38] Lotfi M., Hamblin M.R., Rezaei N.: COVID-19: Transmission, prevention, and potential therapeutic opportunities, *Clinica Chimica Acta*, vol. 508, pp. 254–266, 2020. doi: 10.1016/j.cca.2020.05.044.

[39] Naruei I., Keynia F.: A new optimization method based on COOT bird natural life model, *Expert Systems with Applications*, vol. 183, 115352, 2021. doi: 10.1016/j.eswa.2021.115352.

[40] Parejo J.A., Ruiz-Cortés A., Lozano S., Fernandez P.: Metaheuristic optimization frameworks: a survey and benchmarking, *Soft Computing*, vol. 16, pp. 527–561, 2012. doi: 10.1007/s00500-011-0754-8.

[41] Piotrowski A.P., Napiorkowski M.J., Napiorkowski J.J., Rowinski P.M.: Swarm intelligence and evolutionary algorithms: Performance versus speed, *Information Sciences*, vol. 384, pp. 34–85, 2017. doi: 10.1016/j.ins.2016.12.028.

[42] Rezvanian A., Mehdi Vahidipour S., Sadollah A.: An Overview of Ant Colony Optimization Algorithms for Dynamic Optimization Problems. In: M. Andriychuk, A. Sadollah (eds.), *Optimization Algorithms – Classics and Recent Advances*, IntechOpen, Rijeka, 2023. doi: 10.5772/intechopen.111839.

[43] Şahin İ., Dörterler M., Gökçe H.: Optimization of Hydrostatic Thrust Bearing Using Enhanced Grey Wolf Optimizer, *Mechanika*, vol. 25(6), pp. 480–486, 2019. doi: 10.5755/j01.mech.25.6.22512.

[44] Saib B., Abdessemed M.R., Hocin R., Khoualdi K.: Study of Exploration and Exploitation Mechanisms in Nature Inspired Metaheuristics for Global Optimization. In: M.R. Laouar, V.E. Balas, B. Lejdel, S. Eom, M.A. Boudia (eds.), *12th International Conference on Information Systems and Advanced Technologies "ICISAT 2022"*, pp. 442–453, Springer International Publishing, Cham, 2023. doi: 10.1007/978-3-031-25344-7_41.

[45] Sayed S.A.F., ElKorany A., Sayed S.: Applying hunger game search (HGS) for selecting significant blood indicators for early prediction of ICU Covid-19 severity, *Computer Science*, vol. 24(1), pp. 113–136, 2023. doi: 10.7494/csci.2023.24.1.4654.

[46] Shastri A., Nargundkar A., Kulkarni A.J.: A Brief Review of Socio-inspired Metaheuristics. In: *Socio-Inspired Optimization Methods for Advanced Manufacturing Processes*, pp. 19–29, Springer Series in Advanced Manufacturing, Springer, Singapore, 2021. doi: 10.1007/978-981-15-7797-0_2.

[47] Shial G., Sahoo S., Panigrahi S.: A Nature Inspired Hybrid Partitional Clustering Method Based on Grey Wolf Optimization and JAYA Algorithm, *Computer Science*, vol. 24(3), pp. 361–405, 2023. doi: 10.7494/csci.2023.24.3.4962.

[48] Slowik A., Kwasnicka H.: Evolutionary algorithms and their applications to engineering problems, *Neural Computing and Applications*, vol. 32, pp. 12363–12379, 2020. doi: 10.1007/s00521-020-04832-8.

[49] Stork J., Eiben A.E., Bartz-Beielstein T.: A new taxonomy of global optimization algorithms, *Natural Computing*, vol. 21, pp. 219–242, 2022. doi: 10.1007/s11047-020-09820-4.

[50] Talbi E.G.: *Metaheuristics: from design to implementation*, John Wiley & Sons, 2009. doi: 10.1002/9780470496916.

[51] Tantithamthavorn C., McIntosh S., Hassan A.E., Matsumoto K.: Automated parameter optimization of classification techniques for defect prediction models. In: *ICSE'16: Proceedings of the 38th International Conference on Software Engineering*, pp. 321–332, 2016. doi: 10.1145/2884781.2884857.

[52] Tilahun S.L.: Balancing the Degree of Exploration and Exploitation of Swarm Intelligence Using Parallel Computing, *International Journal on Artificial Intelligence Tools*, vol. 28(03), 1950014, 2019. doi: 10.1142/s0218213019500143.

[53] Visintini A.L., Glover W., Lygeros J., Maciejowski J.: Monte Carlo optimization for conflict resolution in air traffic control, *IEEE Transactions on Intelligent Transportation Systems*, vol. 7(4), pp. 470–482, 2006. doi: 10.1109/tits.2006.883108.

[54] Wang C., Horby P.W., Hayden F.G., Gao G.F.: A novel coronavirus outbreak of global health concern, *The Lancet*, vol. 395(10223), pp. 470–473, 2020. doi: 10.1016/s0140-6736(20)30185-9.

[55] Xing B., Gao W.J.: Imperialist Competitive Algorithm. In: *Innovative Computational Intelligence: A Rough Guide to 134 Clever Algorithms. Intelligent Systems Reference Library*, pp. 203–209, Springer, Cham, 2014. doi: 10.1007/978-3-319-03404-1_15.

[56] Yang X.S.: *Nature-inspired metaheuristic algorithms*, Luniver Press, 2010.

[57] Yang X.S., He X.: Swarm Intelligence and Evolutionary Computation: Overview and Analysis. In: X.S. Yang (ed.), *Recent Advances in Swarm Intelligence and Evolutionary Computation*, Studies in Computational Intelligence, vol. 585, pp. 1–23, Springer, Cham, 2015. doi: 10.1007/978-3-319-13826-8_1.

[58] Yin S., Luo Q., Du Y., Zhou Y.: DTSMA: Dominant swarm with adaptive t-distribution mutation-based slime mould algorithm, *Mathematical Biosciences and Engineering*, vol. 19(3), pp. 2240–2285, 2022. doi: 10.3934/mbe.2022105.

[59] Zhang H., Wang X., Memarmoshrefi P., Hogrefe D.: A survey of ant colony optimization based routing protocols for mobile ad hoc networks, *IEEE Access*, vol. 5, pp. 24139–24161, 2017. doi: 10.1109/access.2017.2762472.

Appendix

A. Tables

Table A1
Algorithms setting

Algorithm	Settings
ABC	Number of Onlooker Bees=population size Trial Limit=round(0.6*number of desecion variable*population size) Acceleration Coefficient Upper Bound=1
ACO	Sample Size=40 Selection Pressure=0.5 Deviation-Distance Ratio=1
CHIO	Number of solutions have corona virus=1 Spreading rate parameter=0.05
COOT	Number of leaders=ceil(0.1*population size) Number of coot=population size- Number of leaders
COVIDOA	shiftting Number=1 number Of Subprotiens=2 MR=0.1 Gamma=0.5 Beta=0.5
GA	Crossover Percentage=0.7 Number of Offsprings (also Parnets)=2*round(Crossover Percentage*population size/2) Extra Range Factor for Crossover=0.4 Mutation Percentage=0.3 Number of Mutants=round(Mutation Percentage*population size) Mutation Rate=0.1
ICA	Number of Empires/Imperialists=10 Selection Pressure=1 Assimilation Coefficient=1.5 Revolution Probability=0.05 Revolution Rate=0.1 Colonies Mean Cost Coefficient=0.2
PSO	Inertia Weight=1 Inertia Weight Damping Ratio=0.99 Personal Learning Coefficient=1.5 Global Learning Coefficient=2 Inertia Weight=1

Table A2 presents the comparative results of CV19T metaheuristic with and without *Attractiveness* and *Consciousness* parameters for specific benchmarks used in the considered research work; these benchmarks are those who support the hypothesis that adding new adequate parameters can increase the dynamic control of the considered meta-heuristic, leading to increase the quality of its solutions.

Numerical values, shown it the Table A2, represent the performance metrics for aforementioned specific benchmarks (F06, F10, F12, F15, F23). For the configuration without *Attractiveness* and *Consciousness*, the results indicate higher values, signifying a larger objective function value in the optimization process (while remembering that it's a matter of minimization problems). In contrast, when *Attractiveness* and *Consciousness* parameters are incorporated, the values notably decrease, indicating improved performance with enhanced control over the metaheuristic's behavior. Authors of this work believe strongly that for the other benchmarks they can obtain the same results but they have to readjust the parameters values, under this new hypothesis, to find more adequate ones.

Table A2
Parameter sensitivity in CV19T: A closer look at
Attractiveness and *Consciousness* effects on specified functions

	F05	F06	F10	F12	F15	F23
Without *Attractiveness* and *Consciousness*	9.99E+02	2.49E+02	**8.88E–16**	1.32E–02	4.16e–04	–9.99E-00
With *Attractiveness* and *Consciousness*	**2,14E+00**	**1.69E–03**	**8.88E–16**	**1.67E–04**	**3.08E–04**	**–1.1E+01**

B. Figures

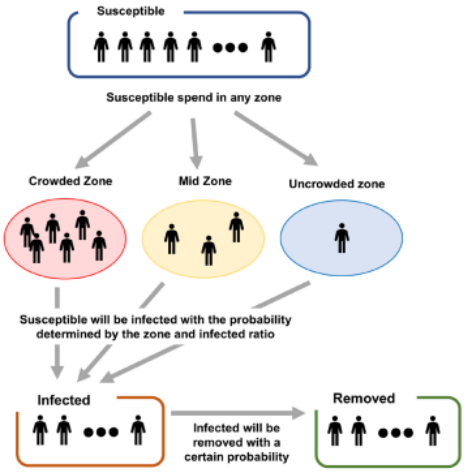

Figure B1. Transition flow between the three compartments: Susceptible, Infected and removed

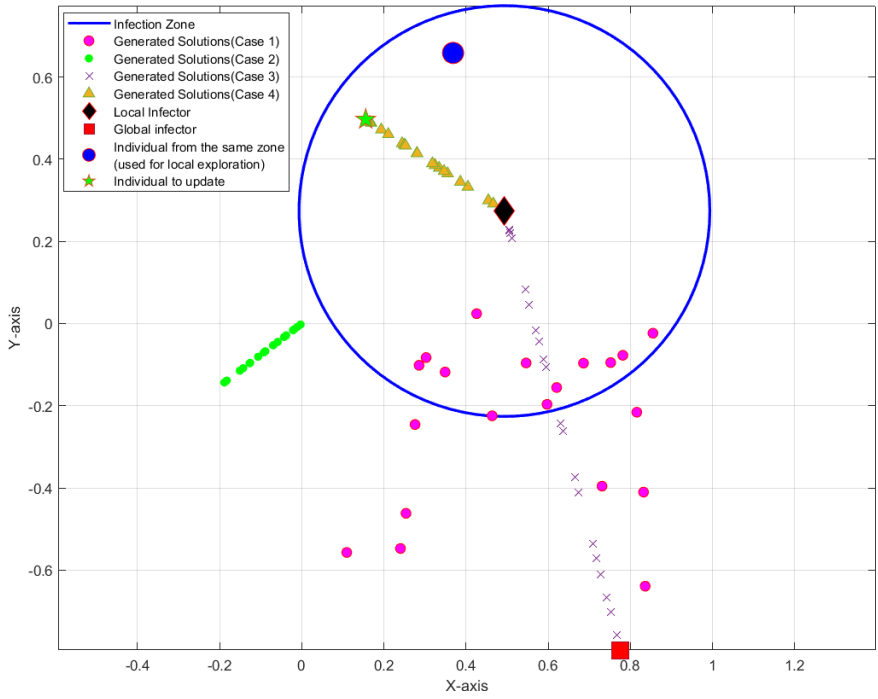

Figure B2. Visualization of the Four Search Strategies in the Proposed Algorithm within a 2D Search Space

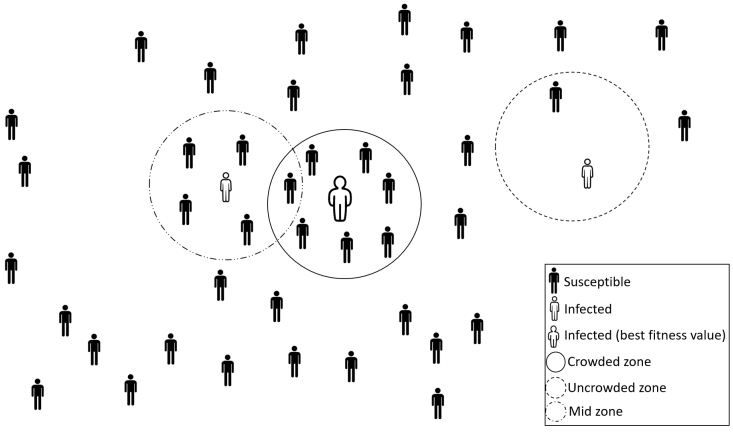

Figure B3. Zone creation

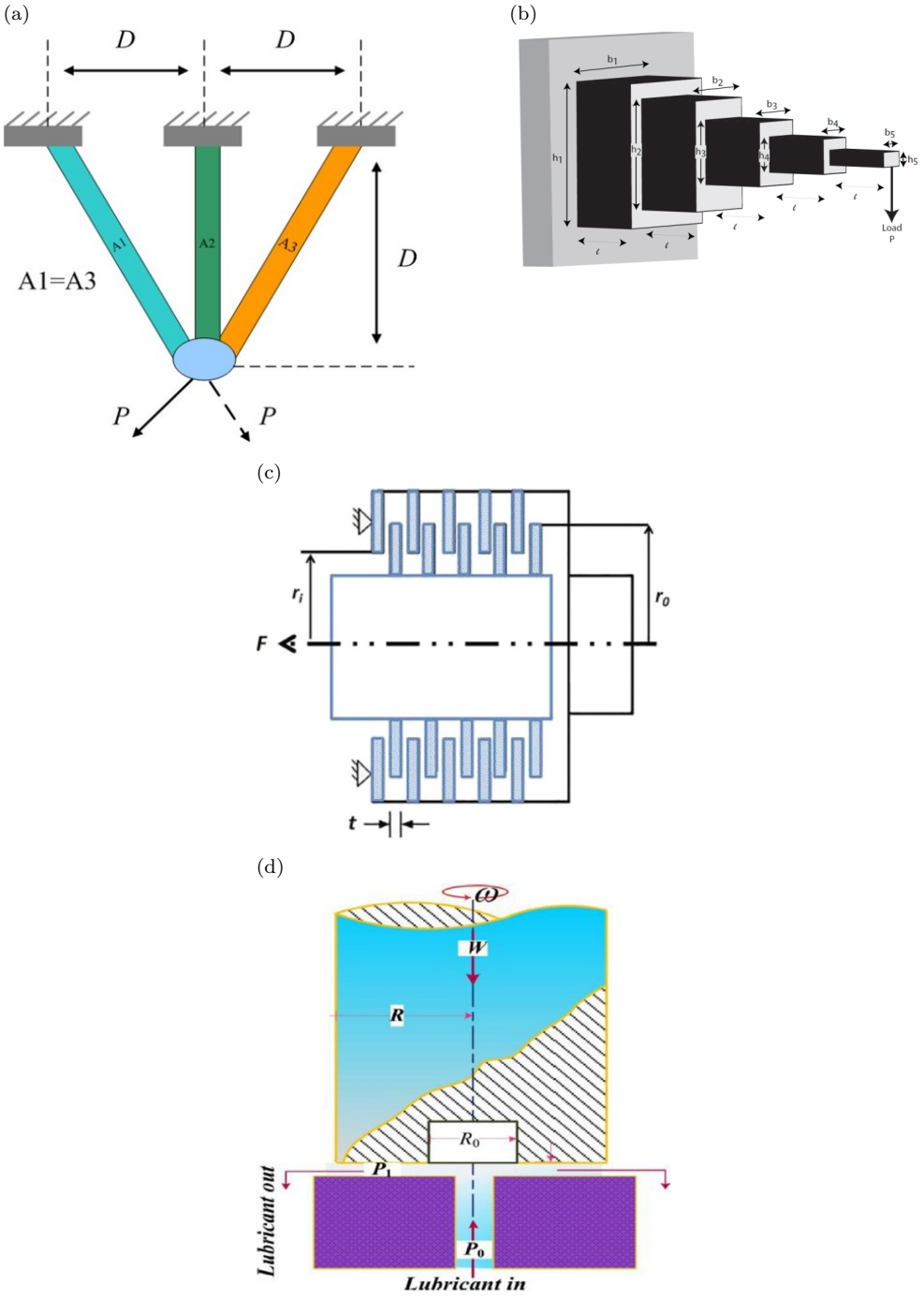

Figure B4. Real-life engineering problems

C. Algorithms

Algorithm C1: Zone creation

```
Initialize distance parameter;
calculate IR using Equation (15);
for i=1:1:IN do
    for j=1:1:populationSize do
        dist=EuclidieanDistance(individial_i, Individual_j)
        if individual_j ≠ individual_i and dist≤IR and individual_j.Zone = 0 then
            individual_j.Zone = individual_i
            individual_j.dist = dist
        else
            if individual_j ≠ individual_i and dist≤IR and dist ≤ individual_j.dist and
              individual_j.Zone ≠ 0 then
                individual_j.Zone = individual_i
                individual_j.dist = dist
            end if
        end if
    end for
end for
for i=1:1:IN do
    BN=the number of individual belonging to individual_i.IR
    if BN ≥ 10 then
        individual_i.ZoneType = CrowdedZone
    else
        if BN ≥ 2 and BN < 10 then
            individual_{i.ZoneType=MidZone}
        else
            individual_i.ZoneType = UncrowdedZone
        end if
    end if
end for
```

Algorithm C2: Update Position

```
if individual_i.Zone = 0 and individual_i.Stat = 0 then
    Case 1;
else
    if individual_i.Stat = 1 then
        Case 3;
    else
        if rand ¡ 0.5 then
            Case 2;
        else
            Case 4;
        end if
    end if
end if
```

Algorithm C3: CV19T

```
Initialization of parameters;
Randomly generate initial population ;
Evaluate initial population;
Return gbest;
Set the IN number of individuals as infected;
// IN is the number of infected individuals

while stop criteria doesn't achieved do
    if (the day ends) then
        for i=1:1:IN do
            if (rand < R_removed) then
                /* R_removed)=10 is the probability of removing infected
                   individuals                                          */
                Remove individual i;
                if (rand < 0.5 then
                    Re-generate individual i randomly;
                else
                    Re-generate individual i surround gBest;
                end if
            end if
            Update infection probabilities;
        end for
        Change the state of the best AIN of the population to "infected";
        // AIN is the added number of infected individuals
    else
        Zones creation;
        Update infection state;
        Update position;
        Evaluation;
        if (IN > PpulationSize/2) then
            Change the state of all individuals to not-infected;
        end if
    end if
end while

Return best solution;
```

D. Benchmark functions

The *Range* parameter represents the Lower and the Upper Bounds of the research area, n represents the dimensions of the function, C represents the nature of the Benchmark (U for unimodal and M for Multimodal) and $F(x^*)$represents the global optimum.

Table D1

Unimodal benchmark functions

Function	Equation	Range	n	C	$F(x)^*$
F1	$\sum_{i=1}^{n} x_i^2$	$[-100, 100]$	30	U	0
F2	$\sum_{i=1}^{n} \lvert x_i \rvert + \prod_{i=1}^{n} \lvert x_i \rvert$	$[-10, 10]$	30	U	0
F3	$\sum_{i=1}^{n} \left(\sum_{j=1}^{i} x_j \right)^2$	$[-100, 100]$	30	U	0
F4	$\max_{1 \le i \le n} \lvert x_i \rvert$	$[-100, 100]$	30	U	0
F5	$\sum_{i=1}^{n-1} \left(100(x_{i+1} - x_i^2)^2 + (x_i - 1)^2 \right)$	$[-30, 30]$	30	U	0
F6	$\sum_{i=1}^{n-1} (\lfloor x_i + 0.5 \rfloor)^2$	$[-100, 100]$	30	U	0
F7	$\sum_{i=1}^{n} i x_i^4 + \mathrm{rand}[0, 1]$	$[-128, 128]$	30	U	0

Table D2

Multimodal benchmark functions

Function	Equation	Range	n	C	$F(x)^*$
F8	$\sum_{i=1}^{n} -x_i \sin(\sqrt{\lvert x_i \rvert})$	$[-500, 500]$	30	M	$-12,569.5$
F9	$\sum_{i=1}^{n} (x_i^2 - 10\cos(2\pi x_i) + 10)$	$[-5.12, 5.12]$	30	M	0
F10	$-20\exp\left(-0.2\sqrt{\frac{1}{n}\sum_{i=1}^{n} x_i^2}\right) - \exp\left(\frac{1}{n}\sum_{i=1}^{n}\cos(2\pi x_i)\right) + 20 + \exp(1)$	$[-32, 32]$	30	M	0
F11	$\frac{1}{4000}\sum_{i=1}^{n} x_i^2 - \prod_{i=1}^{n} \cos\left(\frac{x_i}{\sqrt{i}}\right) + 1$	$[-600, 600]$	30	M	0
F13	$0.1\Big(\sin^2(3\pi x_1) + \sum_{i=1}^{n-1}(x_i - 1)^2\big(1 + \sin^2(3\pi x_{i+1})\big) + (x_n - 1)^2\big(1 + \sin^2(2\pi x_n)\big)\Big) + \sum_{i=1}^{n} u(x_i, 5, 100, 4)$	$[-50, 50]$	30	M	0

Table D3

Fixed-dimensional multimodal benchmark functions

Function	Equation	Range	n	C	$F(x)^*$
F14	$\left(0.002 + \sum_{j=1}^{25} \frac{1}{j + \sum_{i=1}^{2}(x_i - a_{ij})^6}\right)^{-1}$	$[-65,\ 65]$	2	M	1
F15	$\sum_{i=1}^{11} \left(a_i - \frac{x_1(b_i^2 + b_i x_2)}{b_i^2 + b_i x_3 + x_4}\right)^2$	$[-5,\ 5]$	4	M	0.00030
F16	$4x_1^2 - 2.1x_1^4 + \frac{x_1^6}{3} + x_1x_2 - 4x_2^2 + 4x_2^4$	$[-5,\ 5]$	2	M	-1.0316
F17	$\left(x_2 - \frac{5.1x_1^2}{4\pi^2} + \frac{5x_1}{\pi} - 6\right)^2 + 10\left(1 - \frac{1}{8\pi}\right)\cos(x_1) + 10$	$[-5,\ 5]$	2	M	0.398
F18	$\Big(1 + (x_1 + x_2 + 1)^2 \times (19 - 14x_1 + 3x_1^2 - 14x_2 + 6x_1x_2 + 3x_2^2)\Big) \times \Big(30 + (2x_1 - 3x_2)^2 \times (18 - 32x_1 + 12x_1^2 + 48x_2 - 36x_1x_2 + 27x_2^2)\Big)$	–	–	–	–
F19	$-\sum_{i=1}^{4} c_i \exp\left(-\sum_{j=1}^{3} a_{ij}(x_j - p_{ij})^2\right)$	$[-1\ ,\ 3]$	3	M	$-3,86$
F20	$-\sum_{i=1}^{4} c_i \exp\left(-\sum_{j=1}^{6} a_{ij}(x_j - p_{ij})^2\right)$	$[0,\ 1]$	6	M	-3.32
F21	$-\sum_{i=1}^{5} \left((x - a_i)\cdot(x - a_i)^T + c_i\right)^{-1}$	$[0,\ 10]$	4	M	-10.1532
F22	$-\sum_{i=1}^{7} \left((x - a_i)\cdot(x - a_i)^T + c_i\right)^{-1}$	$[0,\ 10]$	4	M	-10.4028
F23	$-\sum_{i=1}^{10} \left((x - a_i)\cdot(x - a_i)^T + c_i\right)^{-1}$	$[0,\ 10]$	4	M	-10.5363

E. Results tables

Table E1
Uni-modal benchmarks results

		CV19T	ABC	ACO	CHIO	COOT	COVIDOA	GA	ICA	PSO
F01	BEST	**0,0000E+00**	5.263E−24	1.000E−05	1.608E−40	**0,0000E+00**	8.104E+00	6.768E−01	3.177E−49	1.156E−121
	MEAN	**0,0000E+00**	1.457E−22	2.676E−05	1.268E+00	1.587E−130	2.023E+01	3.264E+00	6.773E−47	1.357E−21
	WORST	**0,0000E+00**	8.848E−22	7.133E−05	4.014E+00	3.174E−129	3.898E+01	7.344E+00	3.091E−46	2.712E−20
	STD	**0,0000E+00**	2.104E−22	1.602E−05	1.325E+00	7.097E−130	7.674E+00	1.718E+00	9.420E−47	6.064E−21
	H	\	1	1	1	1	0	0	0	1
F02	BEST	**0,0000E+00**	1.210E−29	7.022E−16	2.313E−01	**0,0000E+00**	4.490E−01	1.291E−01	2.570E−31	1.908E−05
	MEAN	**0,0000E+00**	1.940E−28	7.508E−12	3.235E−01	1.309E−258	6.338E−01	3.858E−01	1.039E−28	4.430E−03
	WORST	**0,0000E+00**	7.490E−28	1.327E−10	3.869E−01	2.617E−257	1.141E+00	6.797E−01	1.150E−27	2.472E−02
	STD	**0,0000E+00**	1.970E−28	2.969E−11	4.361E−02	**0,0000E+00**	1.638E−01	1.620E−01	2.693E−28	6.412E−03
	H	\	0	1	0	0	0	0	0	0
F03	BEST	**0,0000E+00**	1.559E+04	4.087E+04	1.866E+03	**0,0000E+00**	9.687E+01	1.152E+02	1.691E−05	4.338E−38
	MEAN	**0,0000E+00**	2.025E+04	6.530E+04	2.815E+03	4,9e-324	3.582E+02	1.900E+02	3.166E−04	6.760E−34
	WORST	**0,0000E+00**	2.453E+04	9.035E+04	4.152E+03	4,9e-323	5.629E+01	1.565E+03	1.367E−03	8.044E−33
	STD	**0,0000E+00**	2.170E+03	1.234E+04	6.765E+02	**0,0000E+00**	2.212E+02	3.460E+03	3.400E−04	2.000E−33
	H	\	1	1	1	0	1	1	1	1
F04	BEST	**0,0000E+00**	4.313E+01	3.506E+00	2.069E+00	**0,0000E+00**	1.079E+00	1.389E+00	1.394E−06	3.030E−19
	MEAN	**0,0000E+00**	4.703E+01	5.747E+00	3.483E+00	1.824E−179	1.569E+00	1.922E+00	4.973E−06	5.371E−17
	WORST	**0,0000E+00**	5.034E+01	1.012E+01	4.985E+00	3.647E−178	2.311E+00	2.372E+00	8.048E−06	2.729E−16
	STD	**0,0000E+00**	2.478E+00	1.838E+00	8.947E−01	**0,0000E+00**	3.436E−01	2.435E−01	2.004E−06	9.494E−17
	H	\	1	1	1	0	1	1	1	1
F05	BEST	**2,3841E−10**	1.940E+01	2.281E+01	2.004E+00	2.121E+01	8.612E+01	1.376E+02	2.250E−02	1.546E−05
	MEAN	**2,1352E+00**	2.057E+01	2.316E+01	8.823E+01	2.274E+01	9.795E+02	3.001E+02	1.714E+01	2.803E+01
	WORST	**2,1365E+01**	2.356E+01	2.347E+01	1.495E+02	2.369E+01	3.296E+03	5.344E+02	7.443E+01	7.464E+01
	STD	6.572E+00	**7,7601E−01**	**1,7523E−01**	4.715E+01	**6,4638E−01**	8.746E+02	1.054E+02	2.773E+01	2.279E+01
	H	\	1	1	1	0	1	0	0	1
F06	BEST	**0,0000E+00**	**0,0000E+00**	7.709E−25	**0,0000E+00**	1.376E−13	1.578E+00	7.459E−01	**0,0000E+00**	9.553E−32
	MEAN	**0,0000E+00**	9.815E−32	6.039E−24	4.122E−01	1.463E−11	4.019E+00	3.102E+00	**0,0000E+00**	1.403E−21
	WORST	**0,0000E+00**	1.196E−30	1.671E−23	8.722E−01	1.295E−10	7.797E+00	6.094E+00	**0,0000E+00**	1.550E−20
	STD	**0,0000E+00**	2.730E−31	4.793E−24	3.257E−01	3.081E−11	1.686E+00	1.686E+00	**0,0000E+00**	4.254E−21
	H	\	0	1	1	1	1	1	1	1
F07	BEST	**4,5388E−07**	2.816E−02	1.170E−02	2.233E−02	1.374E−05	2.298E−03	3.378E−03	3.449E−03	4.497E−04
	MEAN	**6,1099E−06**	4.123E−02	2.067E−02	3.617E−02	1.228E−04	7.662E−03	5.742E−03	6.909E−03	1.353E−03
	WORST	**2,1113E−05**	5.256E−02	3.442E−02	4.936E−02	3.147E−04	1.460E−02	1.280E−02	1.011E−02	2.648E−03
	STD	**5,1119E−06**	8.003E−03	5.757E−03	8.323E−03	7.984E−05	3.303E−03	2.190E−03	1.839E−03	6.151E−04
	H	\	1	1	1	0	1	0	1	0

Table E2
Multi-modal benchmarks results

		CV19T	ABC	ACO	CHIO	COOT	COVIDOA	GA	ICA	PSO
F08	BEST	**−1,257E+04**	−6,691E+03	−5,516E+03	**−1,257E+04**	−1,045E+04	−1,038E+04	−1,150E+04	**−1,257E+04**	−7,713E+03
	MEAN	−1,221E+04	−5,998E+03	−4,676E+03	−1,244E+04	−9,308E+03	−8,473E+03	−1,150E+04	**−1,247E+04**	−6,519E+03
	WORST	−1,113E+04	−5,618E+03	−4,245E+03	−1,220E+04	−8,356E+03	−6,403E+03	−1,067E+04	**−1,231E+04**	−4,712E+03
	STD	4,837E+02	2,581E+02	3,375E+02	1,191E+02	5,255E+02	1,151E+03	2,467E+02	**9,211E+01**	7,927E+02
	H	\	1	1	1	1	1	1	1	1
F09	BEST	**0,000E+00**	1,533E+02	1,901E+02	**0,000E+00**	**0,000E+00**	5,616E+01	2,273E−01	5,684E−14	1,990E+01
	MEAN	**0,000E+00**	1,809E+02	2,127E+02	1,532E−01	1,165E−13	9,021E+01	2,866E+00	9,452E−01	4,472E+01
	WORST	**0,000E+00**	2,003E+02	2,275E+02	6,684E−01	1,990E−12	1,229E+02	5,748E+00	2,985E+00	8,756E+01
	STD	**0,000E+00**	9,820E+00	1,169E+01	2,194E−01	4,474E−13	1,993E+01	1,770E+00	1,140E+00	1,373E+01
	H	\	1	1	1	1	1	1	1	1
F10	BEST	**8,882E−16**	4,441E−15	1,217E−13	2,931E−14	**8,882E−16**	4,621E−01	2,458E−02	2,931E−14	6,839E−14
	MEAN	**8,882E−16**	7,461E−15	7,427E−13	3,618E−02	1,306E−13	7,619E−01	5,128E−01	3,499E−14	1,255E+00
	WORST	**8,882E−16**	7,994E−15	1,720E−12	2,436E−01	2,530E−12	1,310E+00	1,504E+00	4,352E−14	2,739E+00
	STD	**0,000E+00**	1,302E−15	4,694E−13	7,513E−02	5,649E−13	2,185E−01	4,907E−01	5,206E−15	8,025E−01
	H	\	1	1	1	1	1	1	1	0
F11	BEST	**0,000E+00**	**0,000E+00**	**0,000E+00**	9,212E−09	**0,000E+00**	9,895E−01	3,167E−01	**0,000E+00**	**0,000E+00**
	MEAN	**0,000E+00**	**0,000E+00**	2,466E−02	1,173E−01	5,551E−18	1,037E+00	9,047E−01	3.274E−02	1,203E−02
	WORST	**0,000E+00**	**0,000E+00**	2,755E−01	6,971E−01	1,110E−16	1,102E+00	1,054E+00	1,075E−01	7,306E−02
	STD	**0,000E+00**	**0,000E+00**	6,743E−02	2,354E−01	2,483E−17	2,949E−02	1,823E−01	3.262E−02	1,713E−02
	H	\	1	1	1	0	1	1	1	0
F12	BEST	**1,571E−32**	9,926E−28	8,229E−22	1,571E−32	5,569E−16	2,352E−02	3,950E−04	**1,571E−32**	1,651E−32
	MEAN	1,433E−30	2,411E−24	4,110E−18	1,260E−03	1,489E−13	3,009E−01	3,149E−03	**1,571E−32**	8,293E−02
	WORST	1,966E−29	2,497E−23	2,537E−17	2,482E−03	1,645E−12	2,680E+00	1,120E−02	**1,571E−32**	3,110E−01
	STD	4,597E−30	5,857E−24	6,235E−18	9,161E−04	3,724E−13	5,861E−01	2,663E−03	**2,808E−48**	1,095E−01
	H	\	1	1	1	0	0	0	1	0
F13	BEST	**1,350E−32**	1,324E−28	4,634E−20	**1,350E−32**	7,249E−15	1,032E−01	1,949E−02	**1,350E−32**	1,572E−30
	MEAN	1,130E−31	1,178E−26	1,461E−17	3,000E−02	4,507E−12	2,329E−01	1,168E−01	**1,350E−32**	1,342E−01
	WORST	1,061E−30	1,131E−25	1,013E−16	6,177E−02	4,436E−11	4,842E−01	2,671E−01	**1,350E−32**	8,975E−01
	STD	2,616E−31	2,737E−26	2,449E−17	2,262E−02	1,111E−11	1,031E−01	5,912E−02	**2,808E−48**	2,641E−01
	H	\	1	1	1	1	1	1	0	1

Table E3
Fixed dimensional Multi-modal benchmarks results F14–F19

		\	ABC	ACO	CHIO	COOT	COVIDOA	GA	ICA	PSO
F14	BEST	**9.980E–01**	**9.980E–01**	**9.980E–01**	**9.980E–01**	**9.980E–01**	**9.980E–01**	**9.980E–01**	**9.980E–01**	**9.980E–01**
	MEAN	**9.980E–01**	**9.980E–01**	**9.980E–01**	**9.980E–01**	**9.980E–01**	**9.980E–01**	**9.980E–01**	**9.980E–01**	3.216E+00
	WORST	**9.980E–01**	**9.980E–01**	**9.980E–01**	**9.980E–01**	**9.980E–01**	**9.980E–01**	**9.980E–01**	9.980E–01	1.076E+01
	STD	2.038E–16	1.057E–09	**0.000E+00**	6.553E–11	7.204E–17	2.538E–10	4.875E–15	**1.441E–16**	2.580E+00
	H	\	1	1	1	1	1	1	1	1
F15	BEST	**3.075E–04**	3.279E–04	8.352E–04	3.560E–04	**3.075E–04**	3.134E–04	5.430E–04	**3.075E–04**	**3.075E–04**
	MEAN	**3.075E–04**	5.704E–04	1.030E–03	6.517E–04	**3.075E–04**	1.045E–03	8.095E–04	4.043E–04	1.466E–03
	WORST	**3.075E–04**	7.166E–04	1.789E–03	8.419E–04	**3.075E–04**	2.036E–03	1.584E–03	1.223E–03	2.036E–02
	STD	1.380E–09	1.026E–04	2.604E–04	1.240E–04	**2.002E–16**	5.664E–04	2.716E–04	2.809E–04	4.465E–03
	H	\	1	0	1	1	1	0	1	1
F16	BEST	**−1.032E+00**	**−1.032E+00**	**−1.032E+00**	**−1.032E+00**	**−1.032E+00**	**−1.032E+00**	**−1.032E+00**	**−1.032E+00**	**−1.032E+00**
	MEAN	**−1.032E+00**	**−1.032E+00**	**−1.032E+00**	**−1.032E+00**	**−1.032E+00**	**−1.032E+00**	**−1.032E+00**	**−1.032E+00**	**−1.032E+00**
	WORST	**−1.032E+00**	**−1.032E+00**	**−1.032E+00**	**−1.032E+00**	**−1.032E+00**	**−1.031E+00**	**−1.032E+00**	**−1.032E+00**	**−1.032E+00**
	STD	**1.441E–16**	6.234E–13	2.278E–16	4.727E–09	1.765E–16	5.773E–05	3.688E–10	2.100E–16	2.278E–16
	H	\	1	0	0	0	0	0	1	1
F17	BEST	**3.979E–01**	**3.979E–01**	**3.979E–01**	**3.979E–01**	**3.979E–01**	**3.979E–01**	**3.979E–01**	**3.979E–01**	**3.979E–01**
	MEAN	**3.979E–01**	**3.979E–01**	**3.979E–01**	**3.979E–01**	**3.979E–01**	3.980E–01	**3.979E–01**	**3.979E–01**	**3.979E–01**
	WORST	**3.979E–01**	**3.979E–01**	**3.979E–01**	**3.979E–01**	**3.979E–01**	3.985E–01	**3.979E–01**	**3.979E–01**	**3.979E–01**
	STD	**0.000E+00**	8.509E–09	**0.000E+00**	6.750E–08	3.209E–13	1.412E–04	9.324E–10	**0.000E+00**	**0.000E+00**
	H	\	0	0	1	0	1	1	0	0
F18	BEST	**3.000E+00**	**3.000E+00**	**3.000E+00**	**3.000E+00**	**3.000E+00**	**3.000E+00**	**3.000E+00**	**3.000E+00**	**3.000E+00**
	MEAN	**3.000E+00**	**3.000E+00**	**3.000E+00**	**3.000E+00**	**3.000E+00**	3.008E+00	**3.000E+00**	**3.000E+00**	**3.000E+00**
	WORST	**3.000E+00**	**3.000E+00**	**3.000E+00**	**3.000E+00**	**3.000E+00**	3.024E+00	**3.000E+00**	**3.000E+00**	**3.000E+00**
	STD	2.955E–15	9.153E–12	6.280E–16	3.308E–06	1.111E–15	6.744E–03	6.480E–09	1.166E–15	**5.094E–16**
	H	\	0	0	1	1	1	0	0	0
F19	BEST	**−3.863E+00**	**−3.863E+00**	**−3.863E+00**	**−3.863E+00**	**−3.863E+00**	**−3.862E+00**	**−3.863E+00**	**−3.863E+00**	**−3.863E+00**
	MEAN	**−3.863E+00**	**−3.863E+00**	**−3.863E+00**	**−3.863E+00**	**−3.863E+00**	−3.858E+00	**−3.863E+00**	**−3.863E+00**	**−3.863E+00**
	WORST	**−3.863E+00**	**−3.863E+00**	**−3.863E+00**	**−3.863E+00**	**−3.863E+00**	−3.850E+00	**−3.863E+00**	**−3.863E+00**	**−3.863E+00**
	STD	1.750E–15	**1.565E–15**	2.278E–15	7.571E–13	2.152E–15	3.629E–03	3.394E–10	2.258E–15	2.278E–15
	H	\	0	0	1	0	1	0	1	0

Table E4
Fixed dimensional Multi-modal benchmarks results F20–F23

		CV19T	ABC	ACO	CHIO	COOT	COVIDOA	GA	ICA	PSO
F20	BEST	**−3.322E+00**	**−3.322E+00**	**−3.322E+00**	**−3.322E+00**	**−3.322E+00**	−3.247E+00	**−3.322E+00**	**−3.322E+00**	**−3.322E+00**
	MEAN	−3.239E+00	**−3.322E+00**	−3.310E+00	**−3.322E+00**	−3.316E+00	−3.119E+00	-3.292E+00	**−3.322E+00**	−3.280E+00
	WORST	−3.203E+00	**−3.322E+00**	−3.203E+00	**−3.322E+00**	−3.203E+00	−3.016E+00	−3.203E+00	**−3.322E+00**	−3.203E+00
	STD	5.590E−02	**3.379E−16**	3.659E−02	2.228E−08	2.659E-02	7.040E−02	5.282E−02	4.441E−16	5.818E−02
	H	\	0	0	1	1	1	1	1	1
F21	BEST	**−1.015E+01**	**−1.015E+01**	**−1.015E+01**	**−1.015E+01**	**−1.015E+01**	**−1.015E+01**	**−1.015E+01**	**−1.015E+01**	**−1.015E+01**
	MEAN	**−1.015E+01**	**−1.015E+01**	−5.741E+00	**−1.015E+01**	**−1.015E+01**	−6.888E+00	−5.655E+00	**−1.015E+01**	−5.894E+00
	WORST	**−1.015E+01**	**−1.015E+01**	−2.630E+00	**−1.015E+01**	**−1.015E+01**	−2.683E+00	−2.630E+00	**−1.015E+01**	−2.630E+00
	STD	**1.823E−15**	5.603E−15	3.710E+00	1.025E-04	2.038E−15	3.155E+00	3.491E+00	2.305E−15	3.353E+00
	H	\	0	0	1	1	0	1	0	0
F22	BEST	**−1.040E+01**	**−1.040E+01**	**−1.040E+01**	**−1.040E+01**	**−1.040E+01**	**−1.040E+01**	**−1.040E+01**	**−1.040E+01**	**−1.040E+01**
	MEAN	**−1.040E+01**	**−1.040E+01**	−9.117E+00	**−1.040E+01**	**−1.040E+01**	−9.609E+00	−7.323E+00	−9.610E+00	−8.110E+00
	WORST	**−1.040E+01**	**−1.040E+01**	−2.766E+00	**−1.040E+01**	**−1.040E+01**	−5.087E+00	−2.752E+00	−5.088E+00	−2.752E+00
	STD	4.735E-15	5.345E−15	2.685E+00	1.188E−04	**3.993E−15**	1.937E+00	3.527E+00	1.937E+00	3.594E+00
	H	\	1	1	1	1	1	1	1	1
F23	BEST	**−1.054E+01**	**−1.054E+01**	**−1.054E+01**	**−1.054E+01**	**−1.054E+01**	**−1.054E+01**	**−1.054E+01**	**−1.054E+01**	**−1.054E+01**
	MEAN	**−1.054E+01**	**−1.054E+01**	−9.342E+00	**−1.054E+01**	**−1.054E+01**	−7.888E+00	−8.471E+00	−9.596E+00	−7.520E+00
	WORST	**−1.054E+01**	**−1.054E+01**	−2.422E+00	**−1.054E+01**	**−1.054E+01**	−2.871E+00	−2.427E+00	−3.835E+00	−2.427E+00
	STD	5.420E−05	8.252E−15	2.919E+00	2.626E−04	**4.770E−15**	3.073E+00	3.303E+00	2.310E+00	3.840E+00
	H	\	1	1	1	1	1	1	1	1

Table E5
Results of real-life engineering problems

		CV19T	ABC	ACO	CHIO	COOT	COVIDOA	GA	ICA	PSO
TBTD	BEST	**1.864E+02**	**1.864E+02**	**1.864E+02**	**1.864E+02**	**1.864E+02**	**1.864E+02**	**1.864E+02**	**1.864E+02**	**1.864E+02**
	MEAN	**1.864E+02**	**1.864E+02**	**1.864E+02**	**1.864E+02**	**1.864E+02**	**1.864E+02**	**1.864E+02**	**1.864E+02**	**1.864E+02**
	WORST	**1.864E+02**	**1.864E+02**	**1.864E+02**	**1.864E+02**	**1.864E+02**	**1.864E+02**	1.865E+02	**1.864E+02**	**1.864E+02**
	STD	8.477E–14	1.485E–06	**4.747E–14**	2.169E–03	6.745E–14	4.641E–03	2.190E–02	1.075E–13	5.257E–14
	H	\	1	1	0	1	1	1	1	1
SCBD	BEST	**9.477E+19**	**9.477E+19**	**9.477E+19**	**9.477E+19**	**9.477E+19**	**9.477E+19**	**9.477E+19**	**9.477E+19**	**9.477E+19**
	MEAN	**9.477E+19**	**9.477E+19**	**9.477E+19**	**9.477E+19**	**9.477E+19**	**9.477E+19**	**9.477E+19**	**9.477E+19**	**9.477E+19**
	WORST	**9.477E+19**	**9.477E+19**	**9.477E+19**	**9.477E+19**	**9.477E+19**	**9.477E+19**	**9.477E+19**	**9.477E+19**	**9.477E+19**
	STD	1.638E+04	1.681E+04	1.681E+04	**1.595E+04**	1.681E+04	1.638E+04	2,813E+04	1.681E+04	2.024E+04
	H	\	0	0	1	0	0	0	0	0
MDCBD	BEST	**1.010E+07**	2.074E+14	2.074E+14	2.074E+14	2.074E+14	2.798E+14	2.074E+14	2.250E+07	2.074E+14
	MEAN	**1.010E+07**	2.074E+14	2.074E+14	2.074E+14	2.074E+14	4.401E+14	2.074E+14	2.264E+07	2.074E+14
	WORST	**1.010E+07**	2.074E+14	2.074E+14	2.074E+14	2.074E+14	8.038E+14	2.074E+14	2.276E+07	2.074E+14
	STD	**0.000E+00**	6.412E–02	6.412E–02	6.412E–02	6.412E–02	1.296E+14	6,412E–02	1.019E+05	6.412E–02
	H	\	1	1	1	1	1	1	1	1
HTBD	BEST	2.365E+11	2.365E+11	2.365E+11	2.365E+11	2.365E+11	2.365E+11	2,365E+11	**2.363E+11**	2.365E+11
	MEAN	**2.365E+11**	**2.365E+11**	**2.365E+11**	**2.365E+11**	**2.365E+11**	**2.365E+11**	6,471E+11	1.307E+12	3.605E+11
	WORST	**2.365E+11**	**2.365E+11**	**2.365E+11**	**2.365E+11**	**2.365E+11**	**2.365E+11**	2,759E+12	2.736E+12	2.716E+12
	STD	**6.262E–05**	**6.262E–05**	**6.262E–05**	**6.262E–05**	**6.262E–05**	**6.262E–05**	8,673E+11	1.215E+12	5.545E+11
	H	\	0	0	1	0	0	0	0	0

F. Results curves

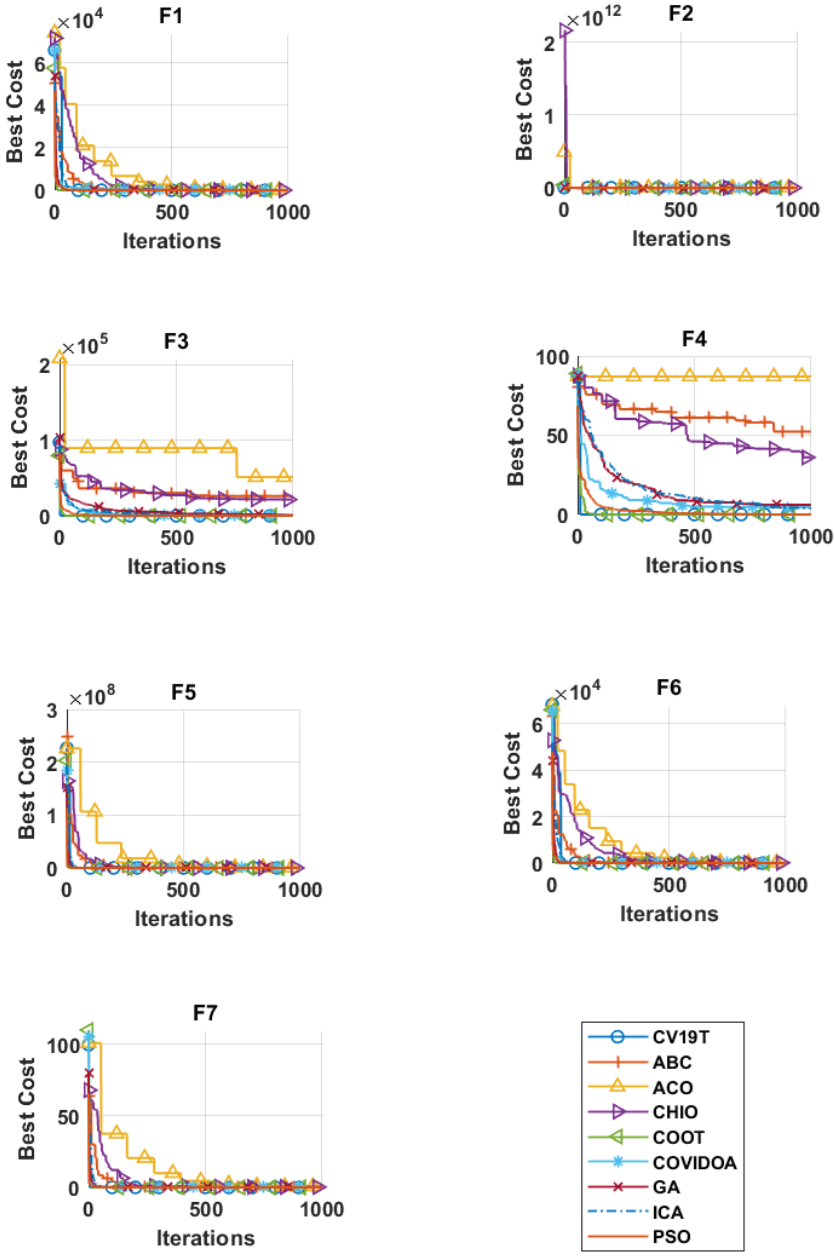

Figure F1. Uni-Modal benchmark functions convergence curves

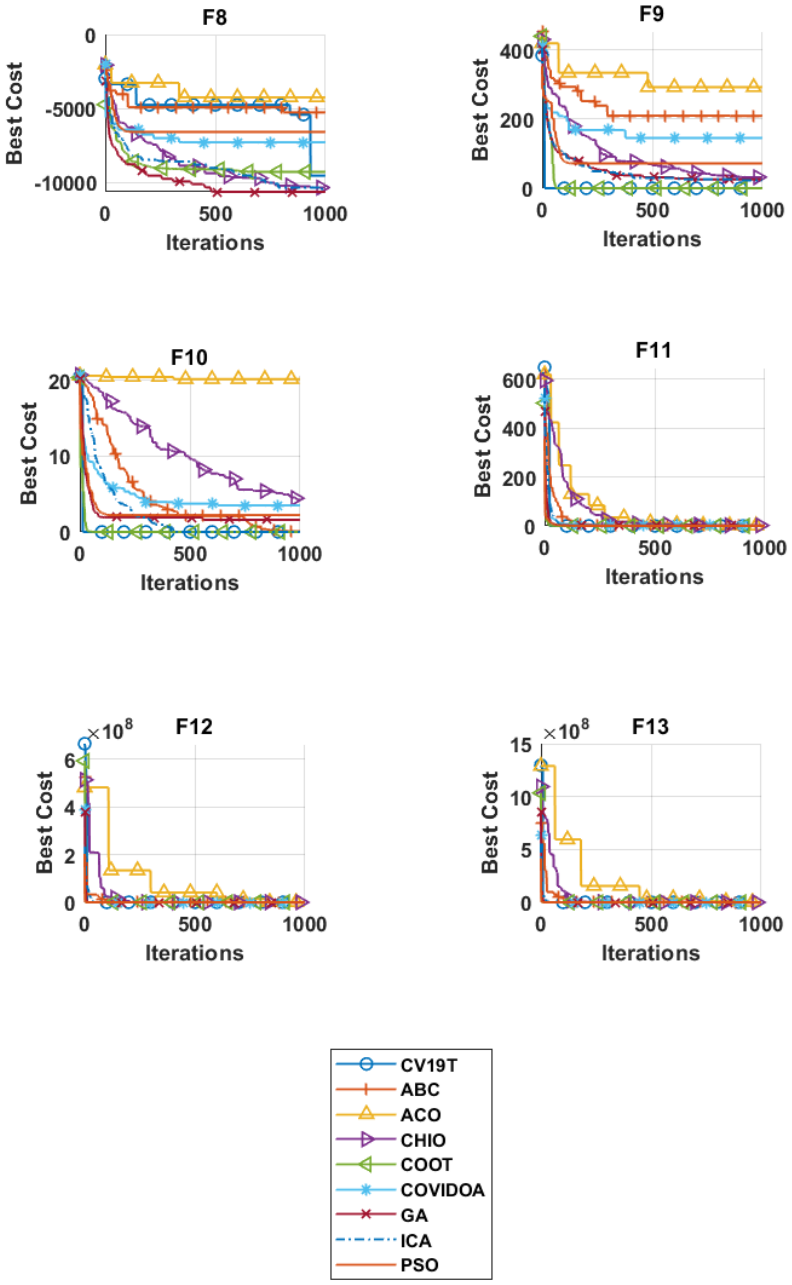

Figure F2. Multi-modal benchmark functions convergence curves

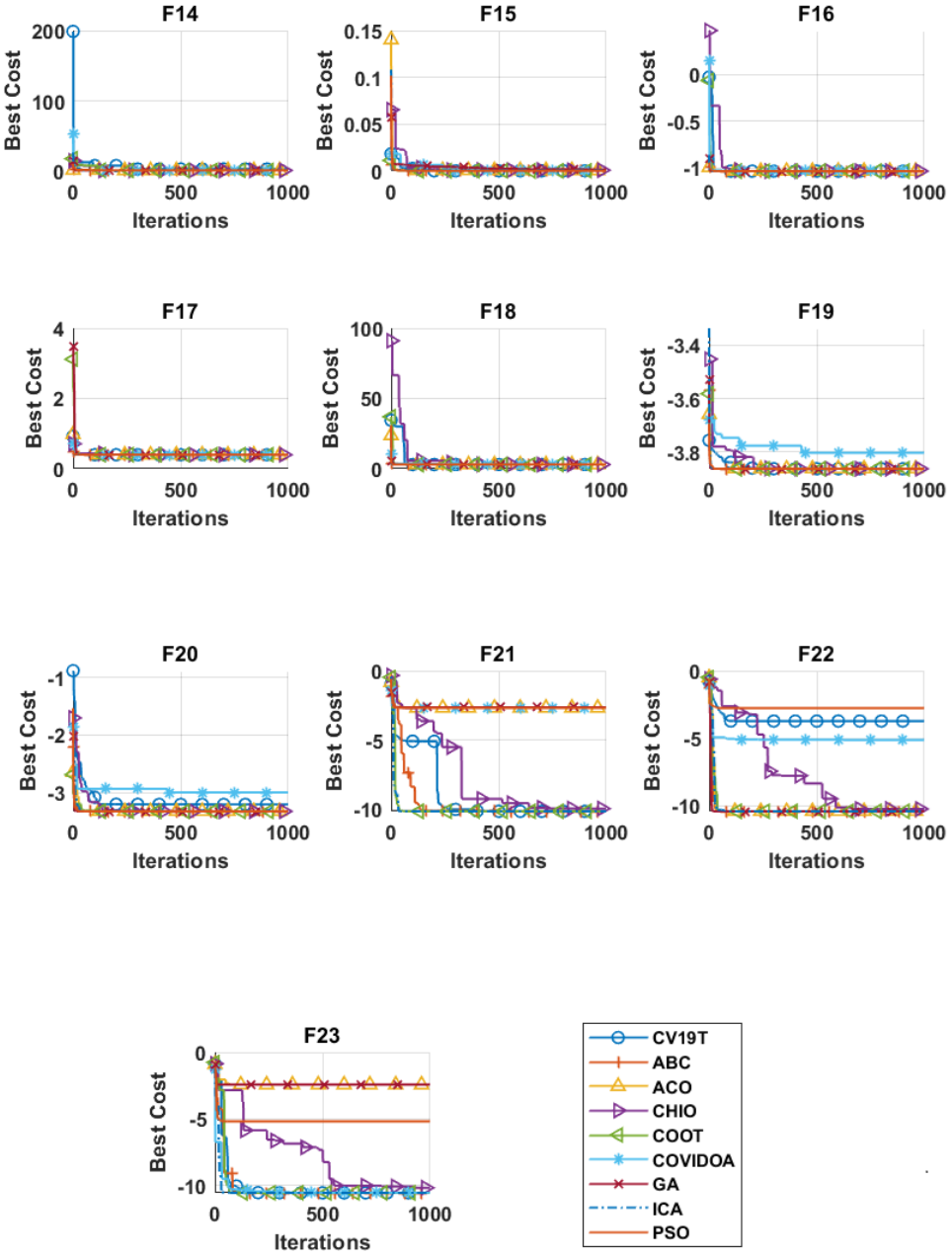

Figure F3. Fixed-dimension multimodal benchmark functions convergence curves

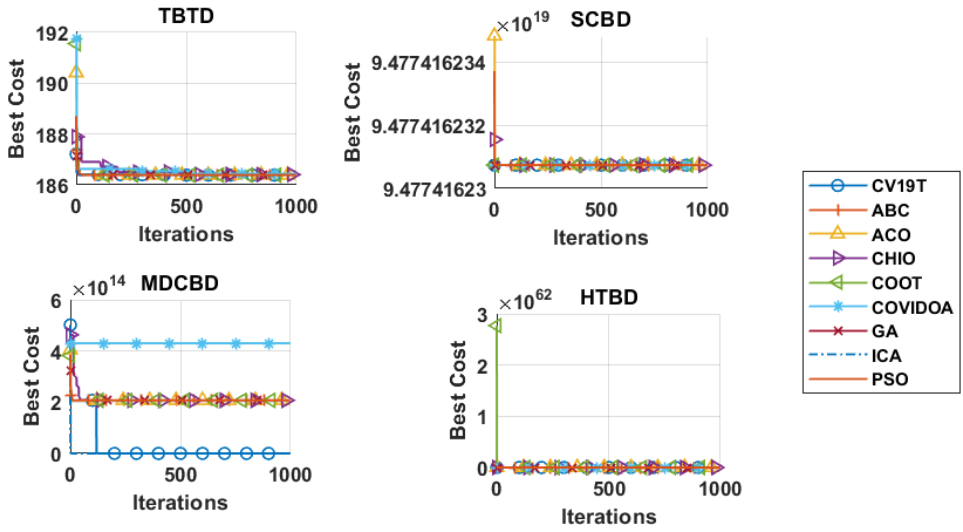

Figure F4. Real-life engineering problems functions convergence curves

Affiliations

Saib Bouthina
Mustapha Ben Boulaid University, Computer Science Departement, Mathematics and Computer Science Faculty, Batna, Algeria, b.saib@univ-batna2.dz

Mohamed-Rida Abdessemed
Mustapha Ben Boulaid University, LAMIE laboratory, Computer Science Departement, Mathematics and Computer Science Faculty, Batna, Algeria, r.abdessemed@univ-batna2.dz

Riadh Hocine
Mustapha Ben Boulaid University, Computer Science Departement, Mathematics and Computer Science Faculty, Batna, Algeria, riadh.hocine@univ-batna2.dz

Received: 6.10.2023
Revised: 25.03.2024
Accepted: 25.03.2024